The Geological Society of America
Special Paper 438
2008

Chronology of pluton emplacement and regional deformation in the southern Sierra Nevada batholith, California

J.B. Saleeby
Division of Geological and Planetary Sciences, California Institute of Technology, Pasadena, California 91125, USA

M.N. Ducea
Department of Geosciences, University of Arizona, Tucson, Arizona 85721, USA

C.J. Busby
Department of Geosciences, University of California, Santa Barbara, California 93106, USA

E.S. Nadin
Division of Geological and Planetary Sciences, California Institute of Technology, Pasadena, California 91125, USA

P.H. Wetmore
Department of Geology, University of South Florida, Tampa, Florida 33620, USA

ABSTRACT

Cretaceous plutonic rocks of the southern Sierra Nevada batholith between latitudes 35.5°N and 36°N lie in a strategic position that physically links shallow, subvolcanic levels of the batholith to lower-crustal (~35 km deep) batholithic rocks. This region preserves an oblique crustal section through the southern Sierra Nevada batholith. Prior studies have produced large U/Pb zircon data sets for an aerially extensive region of the batholith to the north of this area and for the lower-crustal rocks of the Tehachapi complex to the south. We present a large set of new U/Pb zircon age data that ties together the temporal relations of pluton emplacement and intra-arc ductile deformation for the region. We define five informal intrusive suites in the area based on petrography, structural setting, U/Pb zircon ages, and patterns in initial $^{87}Sr/^{86}Sr$ (Sr_i). Two regionally extensive intrusive suites, the 105–98 Ma Bear Valley suite and 95–84 Ma Domelands suite, underlie the entire southwestern and eastern regions of the study area, respectively, and extend beyond the limits of the study area. A third regionally extensive suite (101–95 Ma Needles suite) cuts out the northern end of the Bear Valley suite and extends for an unknown distance to the north of the study area. The Bear Valley and Needles suites are tectonically separated from the Domelands suite by the proto–Kern Canyon fault, which is a regional Late Cretaceous ductile shear zone that runs along the axis of the southern Sierra Nevada batholith. The 105–102 Ma Kern River suite also lies west of the proto–Kern Canyon fault and constitutes the subvolcanic plutonic complex for the 105–102 Ma Erskine Canyon sequence, an ~2-km-thick silicic ignimbrite-

Saleeby, J.B., Ducea, M.N., Busby, C.J., Nadin, E.S., and Wetmore, P.H., 2008, Chronology of pluton emplacement and regional deformation in the southern Sierra Nevada batholith, California, *in* Wright, J.E., and Shervais, J.W., eds., Ophiolites, Arcs, and Batholiths: A Tribute to Cliff Hopson: Geological Society of America Special Paper 438, p. 397–427, doi: 10.1130/2008.2438(14).

hypabyssal complex. The 100–94 Ma South Fork suite lies east of the proto–Kern Canyon fault. It records temporal and structural relations of high-magnitude ductile strain and migmatization in its host metamorphic pendant rocks commensurate with magmatic emplacement.

Integration of the U/Pb age data with structural and isotopic data provides insights into a number of fundamental issues concerning composite batholith primary structure, pluton emplacement mechanisms, compositional variations in plutons, and the chronology and kinematics of regional intra-arc ductile deformation. Most fundamentally, the popular view that Sierran batholithic plutons rise to mid-crustal levels (~20–15 km) and spread out above a high-grade metamorphic substrate is rendered obsolete. Age and structural data of the study area and the Tehachapi complex to the south, corroborated by seismic studies across the shallow-level Sierra Nevada batholith to the north, indicate that felsic batholithic rocks are continuous down to at least ~35 km paleodepths and that the shallower-level plutons, when and if they spread out, do so above steeply dipping primary structures of deeper-level batholith. This steep structure reflects incremental assembly of the lower crust by multiple magma pulses. Smaller pulses at deeper structural levels appear to be more susceptible to having source isotopic and compositional signatures modified by assimilation of partial melt products from metamorphic framework rocks as well as previously plated-out intrusives. Higher-volume magma pulses appear to rise to higher crustal levels without substantial compositional modifications and are more likely to reflect source regime characteristics. There are abundant age, petrographic, and structural data to indicate that the more areally extensive intrusive suites of the study area were assembled incrementally over 5–10 m.y. time scales. Incremental assembly involved the emplacement of several large magma batches in each (~50 km^2-scale) of the larger plutons, and progressively greater numbers of smaller batches down to a myriad of meter-scale plutons, and smaller dikes. The total flux of batholithic magma emplaced in the study area during the Late Cretaceous is about four times that modeled for oceanic-island arcs.

Integration of the U/Pb zircon age data with detailed structural and stratigraphic studies along the proto–Kern Canyon fault indicates that east-side-up reverse-sense ductile shear along the zone was operating by ca. 95 Ma. Dextral-sense ductile shear, including a small reverse component, commenced at ca. 90 Ma and was in its waning phases by ca. 83 Ma. Because ~50% of the southern Sierra Nevada batholith was magmatically emplaced during this time interval, primarily within the east wall of the proto–Kern Canyon fault, the total displacement history of the shear zone is poorly constrained. Stratigraphic relations of the Erskine Canyon sequence and its relationship with the proto–Kern Canyon fault suggest that it was ponded within a 102–105 Ma volcano-tectonic depression that formed along the early traces of the shear zone. Such structures are common in active arcs above zones of oblique convergence. If such is the case for the Erskine Canyon sequence, this window into the early history of the "proto–Kern Canyon fault" could preserve a remnant or branch of the Mojave–Snow Lake fault, a heretofore cryptic hypothetical fault that is thought to have undergone large-magnitude dextral slip in Early Cretaceous time. The changing kinematic patterns of the proto–Kern Canyon fault are consistent with age and deformational relations of ductile shear zones present within the shallow-level central Sierra Nevada batholith, and with those of the deep-level exposures in the Tehachapi complex. This deformational regime correlates with flat-slab segment subduction beneath the southern California region batholithic belt and resultant tilting and unroofing of the southern Sierra Nevada batholith oblique crustal section. These events may be correlated to the earliest phases of the Laramide orogeny.

Keywords: geochronology, tectonics, Sierra Nevada batholith.

INTRODUCTION

Composite batholithic belts of the Cordilleran-type constitute the raw materials of continental crust. The "subduction factory" model for the generation of such belts along active continental margins provides a kinematic and dynamic framework for the interpretation and modeling of tectonic and petrogenetic processes attendant to batholith belt genesis. Recent studies in batholith belt generation (cf. Kay and Kay, 1991; Coleman and Glazner, 1998; Ducea and Saleeby, 1998; Ducea, 2001; Saleeby et al., 2003) indicate that the attendant petrogenetic processes and related large-volume material fluxes occur over vertical length scales that greatly exceed the thickness of typical continental crust. This amplifies the problems of batholith belt structure and petrogenesis, since most Phanerozoic belts are exposed to depth levels that rarely exceed half the thickness of typical continental crust. As a result, there has been a recent focus on the relatively few number of lower-crustal exposures that have thus far been resolved around the circum-Pacific belt of Phanerozoic batholiths (Saleeby, 1990; Barth and May, 1992; Pickett and Saleeby, 1993, 1994; Klepeis et al., 2003; Kidder et al., 2003; Paterson et al., 2008). Such studies are essential in gaining a fuller understanding of batholith belt genesis, and for elucidating criteria for recognition of lower batholithic crust. One key to relating what is learned from such lower-crustal exposures to whole-crust-scale process lies in resolving consanguineous rock sequences that physically link lower- and upper-crustal domains. This paper focuses on providing such a linkage for an oblique crustal section through the southernmost Sierra Nevada batholith.

The Sierra Nevada batholith is perhaps the most intensively studied batholithic belt in the world (cf. Evernden and Kistler, 1970; Bateman, 1983; Saleeby, 1990; Sisson et al., 1996; Coleman and Glazner, 1998; Ducea and Saleeby, 1998; Ducea, 2001). This sparse sampling of Sierra Nevada batholith references reflects a few of the many topical and synthesis-type papers that have been published. These have benefited from, and to a great extent were made possible by, systematic quadrangle mapping by the U.S. Geological Survey between latitudes 36.25°N and 38.25°N. Such field mapping facilitated a later generation of intensive regional efforts in geochronology and igneous barometric determinations of pluton emplacement depths, which are discussed in some depth below. These studies have in turn allowed us to ask fundamental questions concerning batholith belt structure and petrogenesis.

Regional geochronological studies indicate that batholithic magmatism was initiated in the Sierra Nevada as early as ca. 248 Ma, continued semicontinuously through much of the Mesozoic, and culminated with its highest volume production in the 85–100 Ma time interval (Evernden and Kistler, 1970; Saleeby and Sharp, 1980; Stern et al., 1981; Saleeby et al., 1987, 1990; Chen and Moore, 1982; Coleman et al., 2004). These studies show clear temporal and spatial patterns in the loci of magmatism, expressed most clearly by a general west-to-east migration of pluton emplacement through the Cretaceous. Superimposed on this longitudinal age zonation pattern, there is an along-strike depth-of-exposure gradient, where regionally continuous shallow-level batholithic rocks (<10 km emplacement depths) grade continuously into deep-level exposures (~35 km) of the Tehachapi complex at the southern end of the range (Ague and Brimhall, 1988; Pickett and Saleeby, 1993; Ague, 1997; Nadin and Saleeby, this volume). Up to this point, extensive U/Pb zircon geochronological data sets have been presented for a large area of the shallow-level exposures to the north of the study area (Saleeby and Sharp, 1980; Stern et al., 1981; Chen and Moore, 1982; Saleeby et al., 1990; Tobisch et al., 1995; Coleman et al., 2004), and also the Tehachapi complex to the south (Saleeby et al., 1987, 2007; Pickett and Saleeby, 1994). However, in the area leading into the steepest longitudinal depth-of-exposure gradient, a critical data gap has existed. In this paper, we fill this gap.

The U/Pb zircon data presented in this paper are tied to regional and detailed mapping, thus facilitating a number of important tectonic and petrogenetic pursuits. We may now track pluton emplacement patterns in time and space over nearly a complete sialic crustal column interval, as well as study the temporal patterns of deformation along a whole-crust-penetrating shear/fault zone. The strategy employed in this study entails two major tracks. First, high-precision U/Pb zircon ages were obtained by isotope dilution procedures on multiple zircon fractions commensurate with a decadal effort in systematic and topical mapping along an ~30-km-wide corridor of the axial Sierra Nevada batholith between latitudes 35.25°N and 36.15°N. The structural and geochronological relations established by this effort were then complemented by a recent regional-scale effort in zircon geochronology utilizing laser-ablation multicollector–inductively coupled plasma–mass spectrometric (LA-MC-ICP-MS) techniques (Kidder et al., 2003; Dickinson and Gehrels, 2003). This rapid analytical technique has facilitated a regional-scale consolidation of the structural and age relations established in the first track. In the following text, we first give an overview of the major tectonic and petrologic features of the southern Sierra Nevada batholith, from a geochronological perspective, present a detailed discussion of our new data, and then focus on several key issues in batholith tectonics and petrogenesis.

REGIONAL SETTING OF THE SOUTHERN SIERRA NEVADA BATHOLITH

Geological Relations

A generalized map of the southern Sierra Nevada batholith is given in Figure 1. In addition to serving as an index map, this figure shows some of the regional relations that characterize the Sierra Nevada batholith. The bulk of the batholith is Cretaceous in age, but also shown are early Mesozoic (Triassic and Jurassic) pluton clusters that generally flank the northwest and southeast margins of the principal Cretaceous cluster. The Cretaceous batholith possesses transverse compositional and age gradients, where Early Cretaceous gabbroic to tonalitic plutons are concentrated along it to the west and progressively younger and more granitic plutons

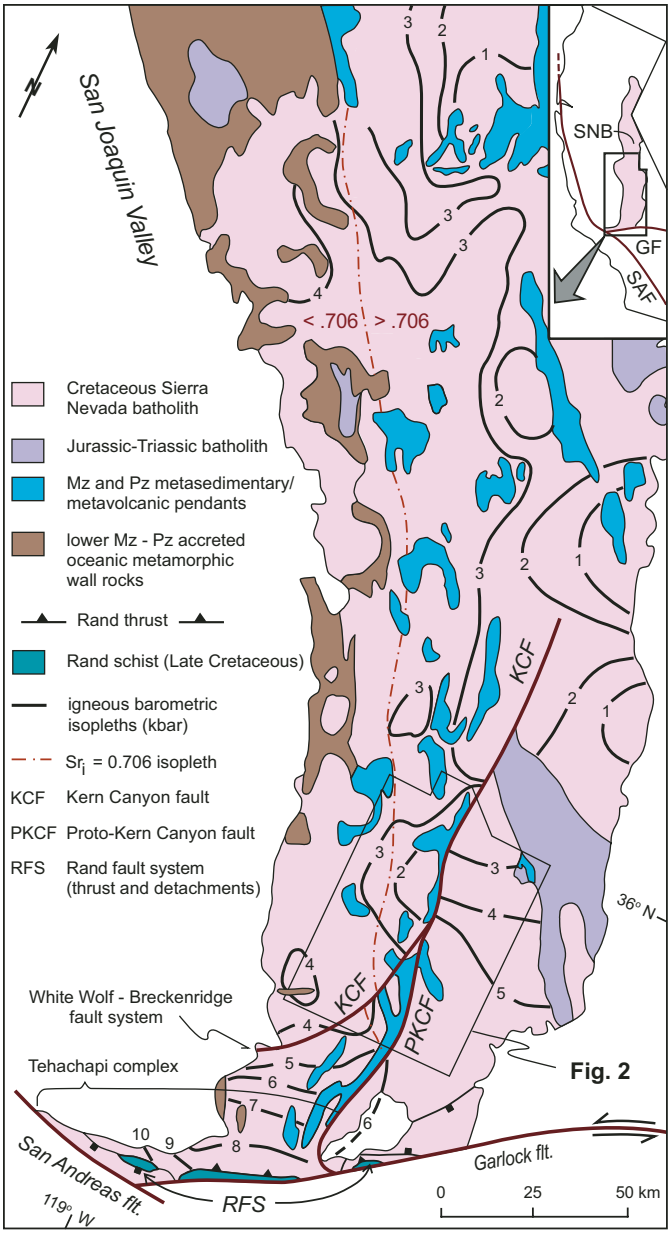

Figure 1. Index map of the southern Sierra Nevada batholith (SNB) showing location of study area (Fig. 2 box), regional-scale lithologic features, Sr_i = 0.706 isopleth (after Kistler, 1990), and igneous barometric isopleths for the Cretaceous (after Ague and Brimhall, 1988; Pickett and Saleeby, 1993; Ague, 1997; Nadin and Saleeby, this volume). GF—Garlock fault, SAF—San Andreas fault, Mz—Mesozoic, Pz—Paleozoic.

occur to the east (cf. Saleeby et al., 2003). The more mafic batholith is for the most part bounded to the east by the Sr_i = 0.706 isopleth (Kistler and Peterman, 1973; Nadin and Saleeby, this volume). The Sr_i = 0.706 isopleth roughly corresponds to a major prebatholithic tectonic break, where prebatholithic rocks to the west formed within a Paleozoic oceanic lithosphere framework, and those to the east formed within a Proterozoic continental lithosphere framework (Saleeby, 1981; Kistler, 1990). Within the study area much of this isopleth corresponds to the proto–Kern Canyon fault, which is a superposed structure relative to the prebatholithic structure.

Figure 2. Generalized geologic map of the study area showing intrusive suites, principal defining plutons, and locations of U/Pb zircon samples. Symbols for plutons studied here are defined in Table 1. Geology is after Saleeby and Busby-Spera (1986), Ross (1989, 1995), and Saleeby and Nadin (2007). Location of Figure 3 geologic map of Erskine Canyon area is shown by box.

The southern Sierra Nevada batholith is cut by three internal, roughly longitudinal shear/fault zones. The proto–Kern Canyon fault is a regionally extensive synbatholithic ductile shear zone that runs along the axis of the southern Sierra Nevada batholith. It has experienced a polyphase history of dextral slip with various components of east-side-up reverse or thrust displacement along its trace (Busby-Spera and Saleeby, 1990; Nadin and Saleeby, this volume). The brittle Kern Canyon fault coincides with the proto–Kern Canyon fault along its northern segment but bifurcates southwestward out of the shear zone at latitude ~35.75°N. (Fig. 2) and continues southwestward to merge with the Breckenridge–White Wolf fault system (Fig. 1). The Kern Canyon fault experienced the terminal phases of synbatholithic dextral slip in association with that of the proto–Kern Canyon fault, as well as superposed Neogene and Holocene normal displacement (Nadin, 2007). The southeastern Sierra Nevada batholith also contains the largely cryptic Kern Plateau shear zone (Dunne and Saleeby, 1993; Behr and Dunne, 2006). This ductile shear zone is shown to have been active primarily in early Mesozoic time, and, in the region of the study area, it is for the most part cut out by Late Cretaceous plutons (Fig. 2).

Superimposed on the transverse zonation pattern of the Cretaceous Sierra Nevada batholith is a longitudinal depth-of-exposure gradient (Ague and Brimhall, 1988; Pickett and Saleeby, 1993; Ague, 1997; Nadin and Saleeby, this volume). This is shown on Figure 1 as a series of isopleths given in 1 kbar contour intervals that denote depth of magmatic emplacement. Much of the central to southern Sierra Nevada batholith may be characterized as having been emplaced at 3 ± 1 kbar crustal levels. Lower pressures of 1–2 kbar are present along part of the eastern Sierra crest, and they represent subvolcanic plutons of Late Cretaceous silicic volcanic sequences. Such a relatively low-pressure domain lies within the study area and is also shown here to represent local subvolcanic levels of the batholith. If the study area is traversed southward from these relatively shallow-level plutons, there is a continuous gradient in depth of exposure, where emplacement depths of ~10 kbar are reached in the Tehachapi complex adjacent to the late Neogene to Holocene Garlock fault. The Garlock fault is interpreted to have preferentially localized along the regional Rand fault system, where it undergoes a major inflection and descends northward from relatively shallow crustal levels to great depths beneath the southernmost Sierra Nevada batholith (Saleeby, 2003). The ~2 to ~10 kbar level of emplacement gradient shown

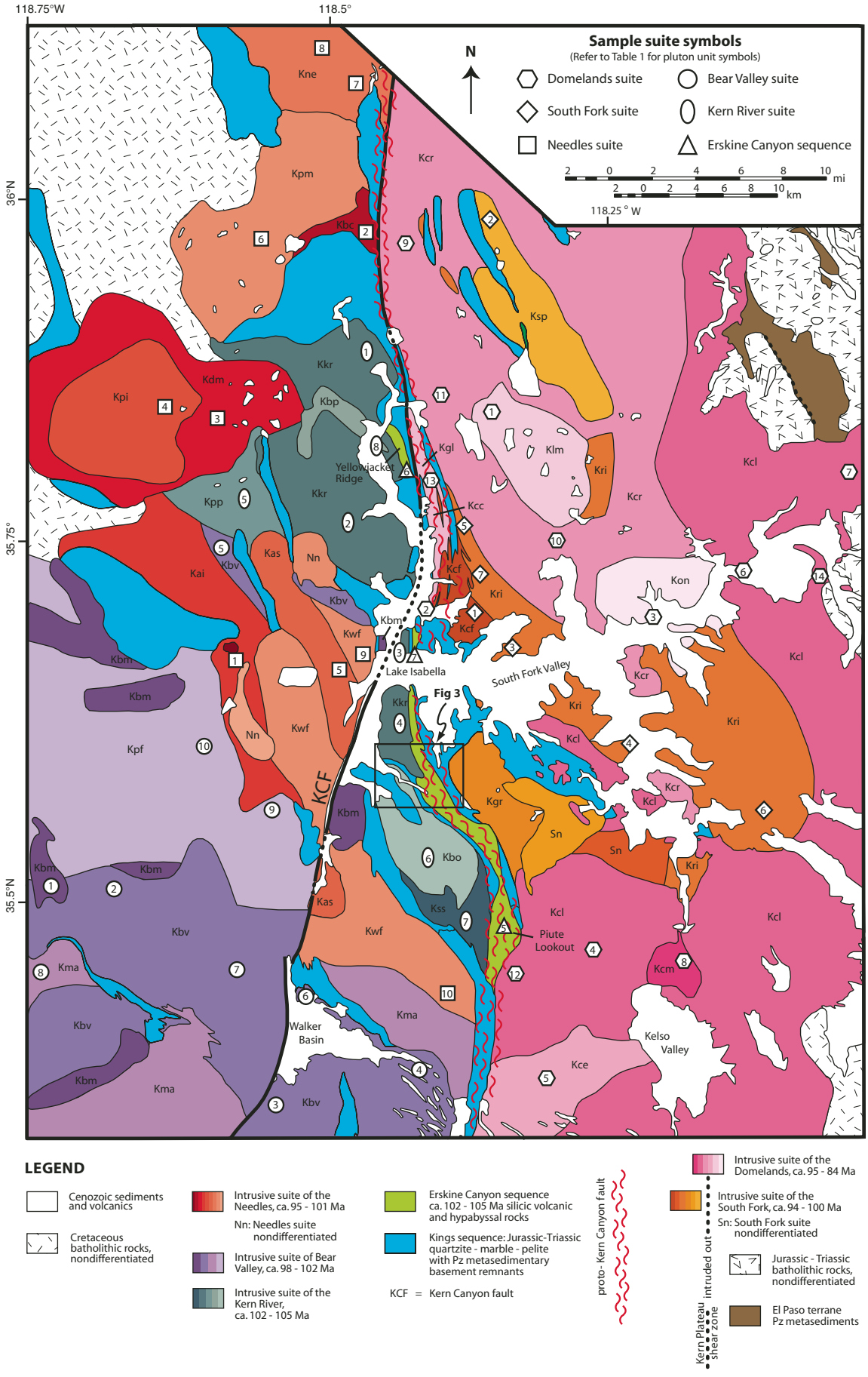
118.75°W
118.5°
36°N
35.75°
35.5°N
118.25 ° W
N
Sample suite symbols
(Refer to Table 1 for pluton unit symbols)
Domelands suite
Bear Valley suite
South Fork suite
Kern River suite
Needles suite
Erskine Canyon sequence
2 0 2 4 6 8 10 mi
2 0 2 4 6 8 10 km
Kne
Kpm
Kbc
Kcr
Ksp
Kkr
Kdm
Kpi
Kbp
Yellowjacket Ridge
Kgl
Klm
Kri
Kcl
Kpp
Kcc
Kas
Nn
Kai
Kbv
Kcf
Kon
Kbm
Kwf
Lake Isabella
South Fork Valley
Fig 3
Kpf
KCF
Kgr
Sn
Kbo
Kss
Piute Lookout
Kcm
Kma
Walker Basin
Kelso Valley
Kce
LEGEND
Cenozoic sediments and volcanics
Cretaceous batholithic rocks, nondifferentiated
Intrusive suite of the Needles, ca. 95 - 101 Ma
Nn: Needles suite nondifferentiated
Intrusive suite of Bear Valley, ca. 98 - 102 Ma
Intrusive suite of the Kern River, ca. 102 - 105 Ma
Erskine Canyon sequence ca. 102 - 105 Ma silicic volcanic and hypabyssal rocks
Kings sequence: Jurassic-Triassic quartzite - marble - pelite with Pz metasedimentary basement remnants
KCF = Kern Canyon fault
proto- Kern Canyon fault
Kern Plateau shear zone intruded out
Intrusive suite of the Domelands, ca. 95 - 84 Ma
Intrusive suite of the South Fork, ca. 94 - 100 Ma
Sn: South Fork suite nondifferentiated
Jurassic - Triassic batholithic rocks, nondifferentiated
El Paso terrane Pz metasediments

for the southernmost Sierra Nevada batholith in Figure 1 traces out an oblique crustal section through the batholith. The principal damage zone of the proto–Kern Canyon fault is observed to flatten eastward at deep levels of the oblique section, and to merge with upper-plate batholithic tectonites of the Rand fault system (Wood and Saleeby, 1998; Nadin and Saleeby, this volume).

Regional Tectonics

This study focuses on the Cretaceous phase of southern Sierra Nevada batholith magmatism. It is widely accepted that the Cretaceous Sierra Nevada batholith was generated above the east-dipping subduction of the Farallon plate beneath SW North America. The adjacent Great Valley and the outboard Franciscan complex represent the coupled forearc basin and exhumed subduction complex, respectively. The west-to-east migration pattern of pluton emplacement in the Sierra Nevada batholith has been attributed to the progressive flattening of the Farallon slab, through Cretaceous time, culminating with the latest Cretaceous to early Paleogene Laramide orogeny (Dickinson and Snyder, 1978). Termination of Sierra Nevada batholith plutonism between ca. 80 and 85 Ma is attributed to such slab flattening and its role in disrupting the delivery of fertile materials to the mantle wedge source of the batholith (Ducea, 2001; Saleeby, 2003). The manner in which Laramide orogeny–related tectonics disrupted Sierra Nevada batholith plutonism changes dramatically along the locus of the batholithic belt. The greater Sierra Nevada batholith mantle lithosphere was left structurally intact, yet "quenched" to a low geotherm following Laramide-related events (Ducea and Saleeby, 1996; Lee et al., 2000; Saleeby et al., 2003). In contrast, structural and age relations at the southern end of the Sierra Nevada batholith and its continuation into the adjacent Southern California batholith indicate that the mantle lithosphere was sheared off at Laramide time, and in-series subduction-accretion assemblages of the Franciscan complex were thrust at low-angle and tectonically underplated as the Rand schist (Malin et al., 1995; Saleeby, 2003; Saleeby et al., 2007). A series of small windows into the schist is shown on Figure 1, along with the Rand fault system, which includes the principal thrust, as well as closely related upper-plate detachment faults (Wood and Saleeby, 1998). Such tectonic relations between the underplated schist and upper-plate(s) batholithic rocks continue southward beneath the Southern California batholith. This north-to-south transition in upper-mantle–lower-crust structure across the southern Sierra Nevada batholith has been attributed to the partitioning of the Farallon plate into a shallow flat segment in the southern California region at Laramide time. In this view, the oblique crustal section of the southernmost Sierra Nevada batholith was unroofed over the slab segmentation inflection zone.

The profound effects of shallow slab segment subduction in general diminish northward along the oblique crustal section. This is broadly expressed by a sharp northward decrease in the intensity of ductile deformation in the Sierra Nevada batholith, as well as brittle structural overprints. One important exception is the northward extension of the proto–Kern Canyon fault. For much of its northern extent, the proto–Kern Canyon fault records synplutonic dextral shear with variable east-side-up reverse/thrust components (Busby-Spera and Saleeby, 1990; Nadin and Saleeby, this volume). To the north, the proto–Kern Canyon fault appears to tie into the Late Cretaceous Sierra Crest shear zone (Tikoff and Teyssier, 1992; Tikoff and St. Blanquat, 1997). This integrated dextral shear system has been likened to major arc-parallel strike-slip faults that develop in active margins experiencing oblique subduction (Busby-Spera and Saleeby, 1990). The Sierra Crest segment of the shear system has been further suggested to have been instrumental in providing space for the Late Cretaceous plutons of the Sierra Nevada batholith (Tikoff and Teyssier, 1992). This is unlikely for much of the southern extent of the proto–Kern Canyon fault, however, as it flattens and increases in its thrust component and thereby severely disrupts the primary structure of the southernmost Sierra Nevada batholith.

MAP RELATIONS AND NOMENCLATURE

Mapping efforts in the study area have consisted of our own regional and detailed topical studies, and regional-scale mapping of Ross (1989, 1995). The detailed studies have focused on the proto–Kern Canyon fault and proximal plutons, and on a number of metamorphic pendants and their hosting plutons. The work of Ross has been instrumental in the designation of major plutonic units based primarily on field petrography and intrusive relations. We adopt and modify the regional pluton nomenclature that was developed by Saleeby et al. (1987) for the Tehachapi complex and subsequently extended northward through the study area and added upon by Ross (1989, 1995). Rocks of the study area to a first order may be broken into Paleozoic-Mesozoic metamorphic pendants, and Cretaceous batholithic rocks. Early Mesozoic members of the Sierra Nevada batholith have been resolved south of latitude 36.4°N only in the extreme southeastern Sierra east of the Kern Plateau shear zone (Fig. 1; Evernden and Kistler, 1970; Dunne and Saleeby, 1993). Early Mesozoic members of the Sierra Nevada batholith are notably lacking in the study area. Next, we briefly discuss the framework pendants of the study area and the batholithic units for which we report U/Pb zircon age data.

Metamorphic Pendants

Metamorphic pendant rocks of the study area were named the Kernville series by Miller and Webb (1940), and metasedimentary rocks were named Long Canyon, Fairview, and the Keene-Tehachapi belt by Ross (1989, 1995). These consist of high-grade quartzite, marble, psammitic and pelitic schist, and subordinate mafic and silicic metavolcanic rocks. They were grouped into the Kings sequence by Saleeby et al. (1978) and Saleeby and Busby (1993), and they correlate to primarily Upper Triassic–Lower Jurassic pendants extending northward from the study area to at least 38°N (Bateman and Clark, 1974). All direct dates on the Kings sequence are of early Mesozoic age. These consist

of marine fossils and U/Pb zircon ages on interbedded silicic ignimbrites. Structural chronological as well as regional tectonic relations suggest the presence of Lower Paleozoic siliciclastic basement vestiges within some of the Kings sequence pendants.

The pendant rocks of the study area are near-pervasive high-strain tectonites. Those dispersed along the proto–Kern Canyon fault consist both of incompletely annealed fault rocks, with variable brittle overprints, and strongly annealed high-strain metamorphic tectonites (Busby-Spera and Saleeby, 1990; Saleeby and Busby, 1993; Nadin and Saleeby, this volume). Those pendants lying outside the proto–Kern Canyon fault are typically high-strain annealed rocks as well, and they have ductile deformation fabrics that record synplutonic deformation commensurate with peak metamorphic equilibration (Saleeby and Busby-Spera, 1986, 1993; Zeng et al., 2005). The age data presented here better constrain the timing of deformation recorded in the pendants. The pattern of high-strain thermal metamorphism pervading the pendant rocks, including those outside the proto–Kern Canyon fault, has one important exception. A domain of relatively shallow pluton emplacement depths occurs west of the proto–Kern Canyon fault between latitudes ~35.5°N and ~35.9°N (Fig. 1). This domain corresponds primarily to the area underlain by the intrusive suite of the Kern River, which is interpreted as a subvolcanic intrusive complex. Thermal metamorphism in the pendant rocks of this domain primarily involved the development of hornfelsic textures with relatively low levels of attendant strain, and thus protolith and prebatholithic deformational features are well preserved. As deeper crustal levels are traversed southward from this shallow-level domain, the thermal overprint recorded in the pendant rocks exhibits progressively more attendant ductile strain, which at its extreme renders anatectic migmatites.

Metamorphic pendants of the study area that lie along the proto–Kern Canyon fault between latitudes 35.46°N and 35.83°N include an unconformable infold of felsic volcanic and hypabyssal rocks (Saleeby and Busby-Spera, 1986). Ross (1989, 1995) referred to these rocks, as well as structurally adjacent high-strain phyllonitic siliciclastic basement rocks within the proto–Kern Canyon fault, as the metavolcanic rocks of French Gulch. Based on our detailed mapping, petrography, and zircon age data, the volcanogenic rocks can for the most part be separated from their underlying basement rocks, and they are shown to be of middle Cretaceous age. The rocks are informally named the Erskine Canyon sequence, based on a well-preserved section where the basal unconformity is preserved in Erskine Canyon (Fig. 3). The Erskine Canyon sequence is shown later in this paper to be closely related to shallow-level plutons of the Kern River intrusive suite.

Intrusive Units

We have grouped most plutons of the study area into five informal intrusive suites (Table 1). Two of the suites are regionally extensive, underlying ~100 × 50 km areas, and consist of numerous bodies emplaced incrementally over ~5–10 m.y. time intervals. These two intrusive suites are completely separated by the proto–Kern Canyon fault, where the Bear Valley suite lies to the west (after Saleeby et al., 1987), and the Domelands suite lies to the east (modified after Ross, 1989).

The Bear Valley suite is predominately tonalitic with subordinate gabbroids and granodiorite. It was originally defined in the deep-level exposures south of the study area. The dominant rock type, tonalite of Bear Valley Springs, extends from ~8 kbar-level exposures in the south continuously for over ~60 km northward into the study area, where it is exposed as shallow as ~2 kbar levels. It is in general bounded to the north by additional shallower-level units of the Bear Valley suite, including the granodiorite of Poso Flat, and the tonalite of Mount Adelaide. The bulk of the Bear Valley suite was intruded over the 98–102 Ma time interval, although members of the suite in the western domains of the Tehachapi complex were intruded as far back as 105 Ma (Pickett and Saleeby, 1994; Saleeby et al., 2007). Throughout its length, the Bear Valley suite contains numerous synplutonic enclaves and commingled dikes of gabbro and diorite, as well as local enclaves of Early Cretaceous (ca. 120–108 Ma) tonalitic intrusions. The entire known north-south extent of the Bear Valley suite is ~120 km. It is at least 50 km in east-west extent, bounded to the east by the proto–Kern Canyon fault and extending well out into the San Joaquin Valley subsurface (Ross, 1989).

The Domelands intrusive suite is predominately granitic-granodioritic in composition; it has large variations in textural features, ranging from K-feldspar megacrystic granite to finer-grained equigranular leuco-granodiorite, mafic granodiorite, aplite, and pegmatite. Many of the more felsic rocks occur as systems of dikes. The Domelands suite was intruded primarily over the 87–93 Ma time interval, although local intrusive sheets and dikes as old as 95 Ma and as young as 83 Ma are included in it.

Additional clusters of apparently related plutons are grouped into three less-extensive suites. Plutons that resemble parts of the Bear Valley suite (Table 1) but are isotopically distinct and are of more limited compositional range (Saleeby et al., 1987; Kistler and Ross, 1990; Pickett and Saleeby, 1994) have been grouped into the Needles intrusive suite. This suite appears to underlie an extensive area to the north of and on strike with the Bear Valley suite, and it extends for an unknown distance beyond the limits of the study area. The Needles suite is also distinguished from the Bear Valley suite by its younger spread of igneous ages (95–101 Ma).

Two less-extensive intrusive suites are defined in the Lake Isabella–Kernville region (Fig. 2). These are completely separated from one another by the proto–Kern Canyon fault. The Kern River suite to the west is a distinct shallow-level intrusive complex characterized primarily by variably textured granite-granodiorite with commingled mafic dike rock. The structural position and age range (102–105 Ma) suggest that this suite is the subvolcanic intrusive complex for the Erskine Canyon volcanic sequence. In addition to its slightly older age range, the Kern River suite has been divided from the Bear Valley suite based on its distinctly more felsic composition, its distinctly shallower-level character, its spatial and temporal association with the Erskine Canyon volcanic sequence, and its distinctly higher range of Sr_i.

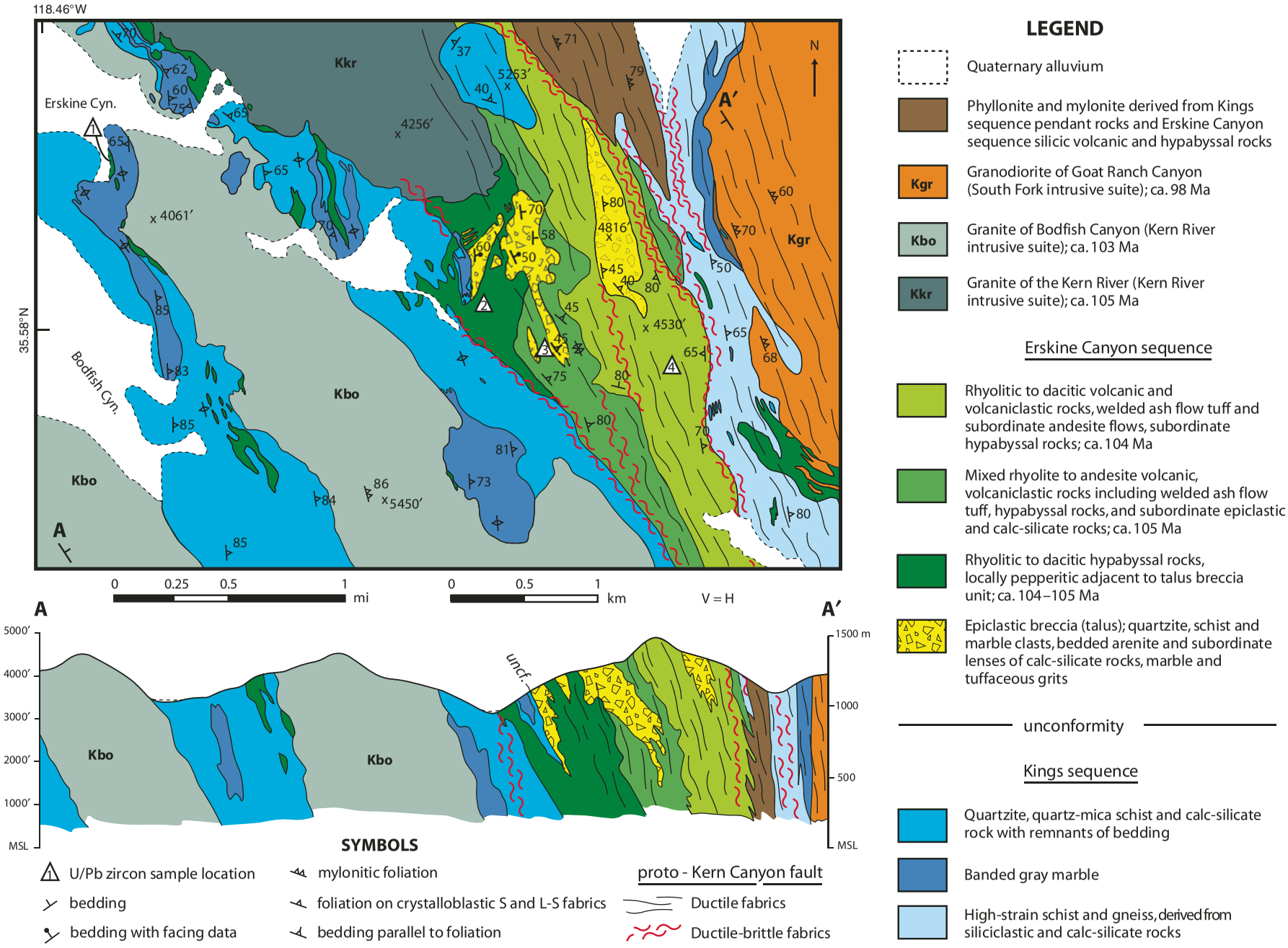

Figure 3. Geologic map of Erskine Canyon area showing relationship between Erskine Canyon sequence and underlying Kings sequence, and the proto–Kern Canyon fault ductile and brittle damage zone (mapping by Saleeby, this paper).

TABLE 1. SUMMARY OF SAMPLE LOCATIONS, NOMENCLATURE, PETROGRAPHY, Sr AND U/Pb ZIRCON AGES

Sample no.	Rock unit	Pluton map symbol†	Lat (°N)	Long (°W)	Petrography	Sr_i	U/Pb zircon age (Ma)
Erskine Canyon Sequence							
E1	Hypabyssal intrusion in Kings sequence quartzite-marble	-	35.592	118.455	Quartz porphyry meta-rhyolite, ground mass hornfelsic	-	104.5 ± 0.4
E2	Pepperitic sill in Kings sequence-derived coarse clastic strata	-	35.588	118.437	Quartz-alkali feldspar porphyry metarhyolite groundmass hornfelsic	-	105.4 ± 1.0
E3	Lower ash flow tuff	-	35.589	118.433	Quartz porphyry rhyolitic lapilli tuff, flattened pumice lapilli 1-10 cm scale, groundmass hornfelsic	-	105.1 ± 0.6
E4	Upper ash flow tuff	-	35.587	118.430	Quartz porphyry rhyolitic tuff, fine stretched lapilli groundmass hornfelsic	0.70637	104.0 ± 0.3
E5	Ash flow tuff within proto–Kern Canyon fault damage zone	-	35.479	118.632	Tectonitic quartz-feldspar porphyry lapilli tuff stretched pumice lapilli up to 50 cm length, schistose groundmass	0.70804	102.2 ± 0.6
E6	Volcanic neck in Kings sequence quartzites	-	35.827	118.443	Plagioclase porphyry dacite breccia, groundmass hornfelsic	-	104.5 ± 0.7
E7	Vestigual lens in proto–Kern Canyon fault	-	35.708	118.431	Quartz porphyry rhylolite, finely phyllonitic groundmass	-	106.5 ± 3.4
Intrusive Suite of the Kern River							
K1	Granite of Kern River	kr	35.875	118.456	K-feldspar-plagioclase-biotite porphyritic granite with fine-grained groundmass	0.70767–0.70812	105.0 ± 0.3
K2	Granite of Kern River	kr	35.770	118.485	Mildly K-feldspar porphyritic granite	0.70767–0.70812	104.3 ± 0.5
K3	Granite of Kern River	kr	35.682	118.443	K-feldspar porphyritic protomylonitic granite	0.70767–0.70812	104.0 ± 1.8
K4	Granite of Kern River	kr	35.615	118.436	K-feldspar porphyritic granite	0.70767–0.70812	104.4 ± 1.7
K5	Granite of Portuguese Pass	pp	35.787	118.570	Coarse-grained biotite granite	0.70852–0.71504	103.2 ± 0.8
K6	Granite of Bodfish Canyon	bo	35.527	118.425	Coarse-grained biotite granite	0.70896	102.8 ± 0.5
K7	Granite of Saddle Springs Road–mafic phase	ss	35.498	118.399	Medium-grained hornblende biotite diorite comingled with granite	0.70608–0.70671	102.5 ± 0.5
K8	Granite of Baker Point	bp	35.825	118.462	Dacitic porphyry dike rock, fine biotite and alkali feldspar phenocrysts		103.1 ± 0.9
Bear Valley Intrusive Suite							
B1	Mafic intrusives commingled with tonalite of Bear Valley Springs	bm	35.478	118.733	Medium-grained hornblende diorite	–	101.8 ± 0.4
B2	Tonalite of Bear Valley Springs	bv	35.507	118.687	Hornblende-biotite tonalite, uncharacteristically poor in mafic enclaves	0.70430	101.0 ± 0.3
B3	Tonalite of Bear Valley Springs	bv	35.351	118.571	Foliated hornblende-biotite tonalite, rich in flattened mafic inclusions	0.70511	100.1 ± 0.7
B4	Tonalite of Bear Valley Springs	bv	35.395	118.435	Foliated-biotite hornblende tonalite, rich in flattened mafic enclaves	0.70425	101.5 ± 0.4
B5	Tonalite of Bear Valley Springs	bv	35.750	118.585	Coarse-grained mafic biotite tonalite	0.70576	102.6 ± 3.9
B6	Early Cretaceous tonalite enclave within tonalite of Bear Valley Springs	–	35.436	118.517	Foliated biotite tonalite with sparse mafic enclaves	–	108.9 ± 1.3
B7	Early Cretaceous tonalite gneiss enclave within tonalite of Bear Valley Springs	–	35.451	118.589	Hornblende-biotite tonalite gneiss	–	113.2 ± 1.0
B8	Tonalite of Mount Adelaide	ma	35.454	118.734	Coarse-grained biotite tonalite with sparse mafic inclusions	0.70449	98.4 ± 0.2
B9	Granodiorite of Poso Flat	pf	35.575	118.566	Coarse-grained biotite tonalite with sparse mafic inclusions	0.70478	100.1 ± 0.3
B10	Granodiorite of Poso Flat	pf	35.603	118.648	Coarse-grained biotite granodiorite poor in mafic inclusions	0.70490	100.2 ± 0.5
Needles Intrusive Suite							
N1	Granodiorite of Alder Creek	al	35.666	118.588	Medium-grained hornblende-biotite granodiorite	0.70638–0.70677	100.9 ± 1.0
N2	Granodiorite of Brush Creek	bc	35.975	118.473	Mafic hornblende granodiorite with abundant mafic inclusions	0.70625	100.6 ± 0.4
N3	Tonalite of Dunlap Meadow	dm	35.826	118.600	Medium-grained hornblende-biotite tonalite	0.70658–0.70714	98.5 ± 0.5
N4	Granodiorite of Pine Flat	pi	35.852	118.626	Medium-grained hornblende-biotite granodiorite	0.70669–0.70742	98.3 ± 0.4
N5	Granodiorite of Alta Sierra	as	35.669	118.486	Fine-grained biotite porphyritic granodiorite	0.70616–0.70653	98.3 ± 3.6
N6	Granodiorite of Peppermint Meadow	pm	35.976	118.569	Medium-grained hornblende-biotite granodiorite	0.70616	97.4 ± 1.5
N7	Granodiorite of the Needles	ne	36.095	118.463	Hornblende-biotite granodiorite with ductile deformation fabric	–	96.8 ± 0.7
N8	"	ne	35.105	118.487	Hornblende-biotite granodiorite	–	96.0 ± 0.5
N9	Granodiorite of Wagy Flat	wf	35.676	118.464	Coarse-grained biotite granodiorite	0.70649–0.70680	95.5 ± 1.2
N10	"	wf	35.426	118.420	Coarse-grained biotite granodiorite	0.70649–0.70680	95.9 ± 1.1
South Fork Intrusive Suite							
S1	Quartz diorite of Cyrus Flat	cf	35.717	118.406	Poikilitic hornblende-hypersthene leucogabbro	0.70677	99.6 ± 0.3
S2	Alaskite of Sherman Pass	sp	35.982	118.359	Coarse-grained hornblende-biotite leucogranodiorite	–	99.3 ± 0.7
S3	Granodiorite of Rabbit Island	ri	35.673	118.353	Medium-grained hornblende-biotite granodiorite, abundant mafic inclusions	0.70593–0.70790	99.0 ± 0.4
S4	Granodiorite of Rabbit Island	ri	35.615	118.249	Medium-grained hornblende-biotite granodiorite, common mafic inclusions	0.70593–0.70790	98.1 ± 0.3
S5	Granodiorite of Rabbit Island	ri	35.578	118.393	Medium-grained hornblende-biotite granodiorite, ductile deformation fabric and stretched mafic inclusions	0.70593–0.70790	97.0 ± 0.4

(*continued.*)

TABLE 1. SUMMARY OF SAMPLE LOCATIONS, NOMENCLATURE, PETROGRAPHY, Sr AND U/Pb ZIRCON AGES (*continued.*)

Sample no.	Rock unit	Pluton map symbol†	Lat (°N)	Long (°W)	Petrography	Sr_i	U/Pb zircon age (Ma)
South Fork Intrusive Suite (*continued.*)							
S6	Granodiorite of Rabbit Island	ri	35.563	118.147	Coarse-grained hornblende-biotite granodiorite, common mafic inclusions	0.70593–0.70790	94.9 ± 0.8
S7	Granodiorite of Rabbit Island	ri	35.729	118.376	Medium-grained hornblende-biotite granodiorite, ductile deformation fabric	0.70593–0.70790	93.7 ± 1.1
Domelands Intrusive Suite							
D1	Granite of Long Meadow	lm	35.848	118.349	Medium-grained biotite granodiorite	–	95.2 ± 0.8
D2	Granite of Cannell Creek	cc	35.709	118.416	Biotite granodiorite mylonite	0.70725–0.70930	94.7 ± 0.4
D3	Granite of Onyx	on	35.701	118.235	Fine-grained biotite-bearing granite	0.70801	93.0 ± 1.5
D4	Granodiorite of Claraville	cl	35.462	118.281	K-feldspar porphyritic biotite granodiorite	0.70751–0.70800	92.5 ± 0.7
D5	Granodiorite of Claraville (equigranular facies)	ce	35.380	118.342	Medium-grained biotite granodiorite-modest planar ductile deformation fabric	0.70704–0.70766	91.9 ± .4
D6	Granodiorite of Claraville	cl	35.741	118.143	K-feldspar porphyritic biotite granodiorite	0.70706	91.2 ± 1.9
D7	"	cl	35.791	118.050	Medium-grained biotite granodiorite	–	90.0 ± 1.9
D8	Granodiorite of Claraville (dark facies)	cm	34.483	118.227	Medium-grained hornblende-biotite granodiorite	–	89.3 ± 0.6
D9	Granite of Castle Rock	cr	35.986	118.443	K-feldspar megacrystic biotite granodiorite protomylonitic	0.70762	89.3 ± 0.2
D10	Granite of Castle Rock	cr	35.744	118.309	Medium-grained biotite-granodiorite	–	89.0 ± 0.5
D11	Granite of Castle Rock	cr	35.857	118.407	Megacrystic K-feldspar biotite granodiorite, mild ductile deformation fabric	–	87.1 ± 0.4
D12	Granodiorite of Claraville, isolated leucogranite dike	–	35.444	118.370	Leucogranite pegmatite	–	86.1 ± 0.4
D13	Granite of Goldledge pegmatite dike swarm	gl	35.801	118.416	Leucogranite pegmatite mylonite	–	85.7 ± 0.5
D14	Granite of Claraville, granite dike swarm	cl	35.736	118.077	Medium-grained biotite hornblende granite	–	84.2 ± 1.5

†Rock unit symbols used on Figure 2 geologic map.

The South Fork intrusive suite is a distinct cluster of small, mainly mafic granodiorite and diorite plutons that straddle the South Fork Valley area east of the proto–Kern Canyon fault (Fig. 2). It was emplaced over the 94–100 Ma time interval at distinctively deeper crustal levels (~5 kbar) than the Kern River suite, situated immediately west of the proto–Kern Canyon fault (Nadin and Saleeby, this volume). The South Fork suite is also distinct in that, during emplacement, its hosting pendant rocks underwent pervasive high-magnitude ductile strain and extensive partial melting along relatively broad high-grade aureoles (Saleeby and Busby-Spera, 1986, 1993; Zeng et al., 2005). Lenses of South Fork suite rocks are transposed along with high-grade pendant rocks within the proto–Kern Canyon fault, and they also occur as widely dispersed enclaves within the Domelands suite. Some of the larger enclaves are shown on Figure 2. Numerous smaller plutonic units occur in the study area but are not differentiated in Figure 2. Many of them have compositional and textural features, as well as contact relations, that are suggestive of affinities to the major intrusive suites defined previously. Except for a series of small plutons belonging to the South Fork suite (Sn and Kgr units, Fig. 2), which have been studied in detail by Zeng (2003), ages have not been determined for these smaller plutons.

U/Pb ZIRCON DATA

We present new U/Pb zircon age data for seven samples of variably metamorphosed silicic ignimbrite and hypabyssal intrusive rock of the Erskine Canyon sequence, and for 47 samples of major plutonic units, and for dikes that bear critical structural relations. The data encompass both detailed and reconnaissance approaches in establishing intrusive and deformational chronologies. Detailed aspects encompass close integration with structural analysis of the proto–Kern Canyon fault, and structural-stratigraphic analysis of the Erskine Canyon sequence. In terms of the aerially extensive plutonic units, this study is a reconnaissance. Our U/Pb zircon data consist of both conventional thermal ionization mass spectrometry (TIMS) isotope-dilution measurements on multiple fractions of small highly purified populations, and laser-ablation ICP-MS analyses on populations of single grains. All grains analyzed by laser ablation were screened by cathodoluminescence (CL) imaging prior to analysis in order to exclude grains with observable older cores or significant inclusions. Tabulated isotopic data as well as a description of the analytical techniques and representative CL images are presented in GSA Data Repository item 2008001.[1]

The isotope-dilution data reveal both discordant and concordant age results. We focus on the relations between $^{206}Pb/^{238}U$ ages and $^{207}Pb/^{206}Pb$ ages to define concordance and discordance. Internal concordance is defined as overlap in these ages, within analytical uncertainty. External concordance is defined by the overlap of these ages within and between multiple fractions. Discordance is defined as disagreement of ages outside of analytical uncertainty. Age assignments of externally concordant samples are based on the error weighted means of the $^{206}Pb/^{238}U$ ages. The topologic relations of concordant and near-concordant age data with concordia are shown by plots of the

[1]GSA Data Repository item 2008001, analytical techniques for isotopic analyses, and supporting data tables and photomicrographs, is available on request from Documents Secretary, GSA, P.O. Box 9140, Boulder, CO 80301-9140, USA, or editing@geosociety.org, and at www.geosociety.org/pubs/ft2008.htm.

error ellipses of the respective data points with the pertinent segments of concordia aligned for the purpose of comparing concordia relations for broadly consanguineous samples within and between spatially associated intrusive suites (Figs. 4, 7, and 8). Treatment of discordant ages is based on concordia intercept theory on $^{207}Pb/^{206}Pb$-$^{238}U/^{206}Pb$ concordia diagrams (Fig. 5) after Tera and Wasserburg (1972). These diagrams are used in lieu of $^{207}Pb/^{235}U$-$^{206}Pb/^{238}U$ diagrams due to the nature of most discordances resolved, which, to a first order, are related to the source inheritance and/or ascent entrainment of primarily Proterozoic zircon. In the general discussion of the data, we do not distinguish between inheritance and entrainment but rather refer to a general "i/e" discordance mechanism. The subject of inheritance versus entrainment is treated in the context of general petrogenetic issues. For the ICP-MS data, we present the results as age-frequency spectra plots (Figs. 6 and 9). The error weighted means of the $^{206}Pb/^{238}U$ ages are used as igneous age assignments. Zircon grains possessing i/e components typically show distinct shifts to older $^{206}Pb/^{238}U$ ages, and these are typically filtered out of the age spectra in calculating the means for the igneous age assignments. The filtered data points are referred to as discordant and are treated in more detail in our petrogenetic discussions.

The zircon age data from the Erskine Canyon sequence is covered first. Next, we cover the data for the batholith in general from oldest to youngest suite and intrasuite pluton emplacement progression, integrating data derived from both analytical techniques. The data are discussed in their geologic context. Two samples, one from the Bear Valley suite (B7) and one from the Domelands suite (D9) were duplicated by both techniques utilized. The igneous age assignments are tabulated in Table 1 along with critical information on sample location, petrography, and available Sr_i. Where the Sr_i data are shown as a range of values, the ranges reflect multiple determinations on numerous samples proximal to the zircon sample location. Table 1 also gives map symbols for plutons that were studied here, as shown on Figure 2.

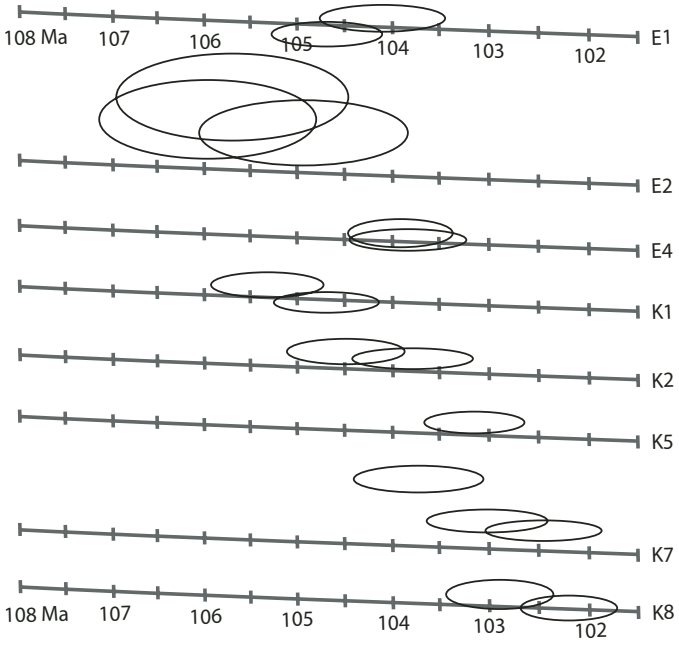

Figure 4. Concordia line segments (after Tera and Wasserburg, 1972) stacked in $^{207}Pb/^{206}Pb$ space for concordant or near-concordant data error ellipses for samples from the Erskine Canyon sequence and Kern River intrusive suite. Errors are 2σ; plotting procedure is modified from Ludwig (2001).

Erskine Canyon Sequence

High-grade siliciclastic-carbonate pendant rocks of the Erskine Canyon area are unconformably overlain and intruded by mid-Cretaceous sedimentary and volcaniclastic rocks and hypabyssal intrusions called the Erskine Canyon sequence (Saleeby and Busby-Spera, 1986). In Erskine Canyon, an ~100–200-m-thick section of quartzite clast breccias and grits with a silty to calcareous matrix, containing calc-silicate rock interbeds unconformably overlies previously deformed marbles and quartzites (Fig. 3). Much of the unconformity is cut out by rhyolitic hypabyssal rocks, which are intruded throughout the breccias, and these commonly bear pepperitic textures and structures. Pepperites are important because they indicate emplacement of the intrusions into clastic sediment while it was still wet and nonlithified (Kokelaar, 1982; Skilling et al., 2004). The breccias and hypabyssals are in turn overlain by rhyolitic to andesitic volcaniclastic rocks that are locally admixed with quartzose detritus. The volcaniclastic rocks include a predominance of silicic ignimbrites that extend southward for ~12 km beyond the Figure 3 map area within the proto–Kern Canyon fault (Fig. 2).

Additional hypabyssal rocks of the Erskine Canyon sequence cut pendant rocks near the mouth of Erskine Canyon (Fig. 3) and ~20 km north of Erskine Canyon along Yellowjacket Ridge (Fig. 2). The Yellowjacket Ridge body appears to represent a volcanic neck. It is characterized by finely recrystallized vitrophyres and complex layering and breccia zones that locally engulf slabs of volcaniclastic rock. Some areas of the neck complex show the effects of intense hydrothermal alteration.

Erskine Canyon sequence rocks are tectonically dispersed relative to one another. A lens of volcanic and hypabyssal rock is sheared out along the proto–Kern Canyon fault northward from the Erskine Canyon area to the north shore area of Lake Isabella (Fig. 2). The Yellowjacket Ridge volcanic neck complex has been further offset 12 ± 1 km in a dextral sense from the Erskine Canyon rocks of the north shore area along the Kern Canyon fault (Nadin and Saleeby, this volume). Furthermore, dextral displacement along the southern segment of the proto–Kern Canyon fault, south of the Kern Canyon fault branching point, is estimated at ~15 km (Nadin and Saleeby, this volume). Much of this displacement was dispersed as dextral shear within the Erskine Canyon sequence and its underlying metasedimentary basement rocks between latitudes 35.45°N and 35.6°N (Figs. 2 and 3).

Preliminary U/Pb zircon ages were presented for some of the Erskine Canyon samples in Saleeby and Busby-Spera (1986).

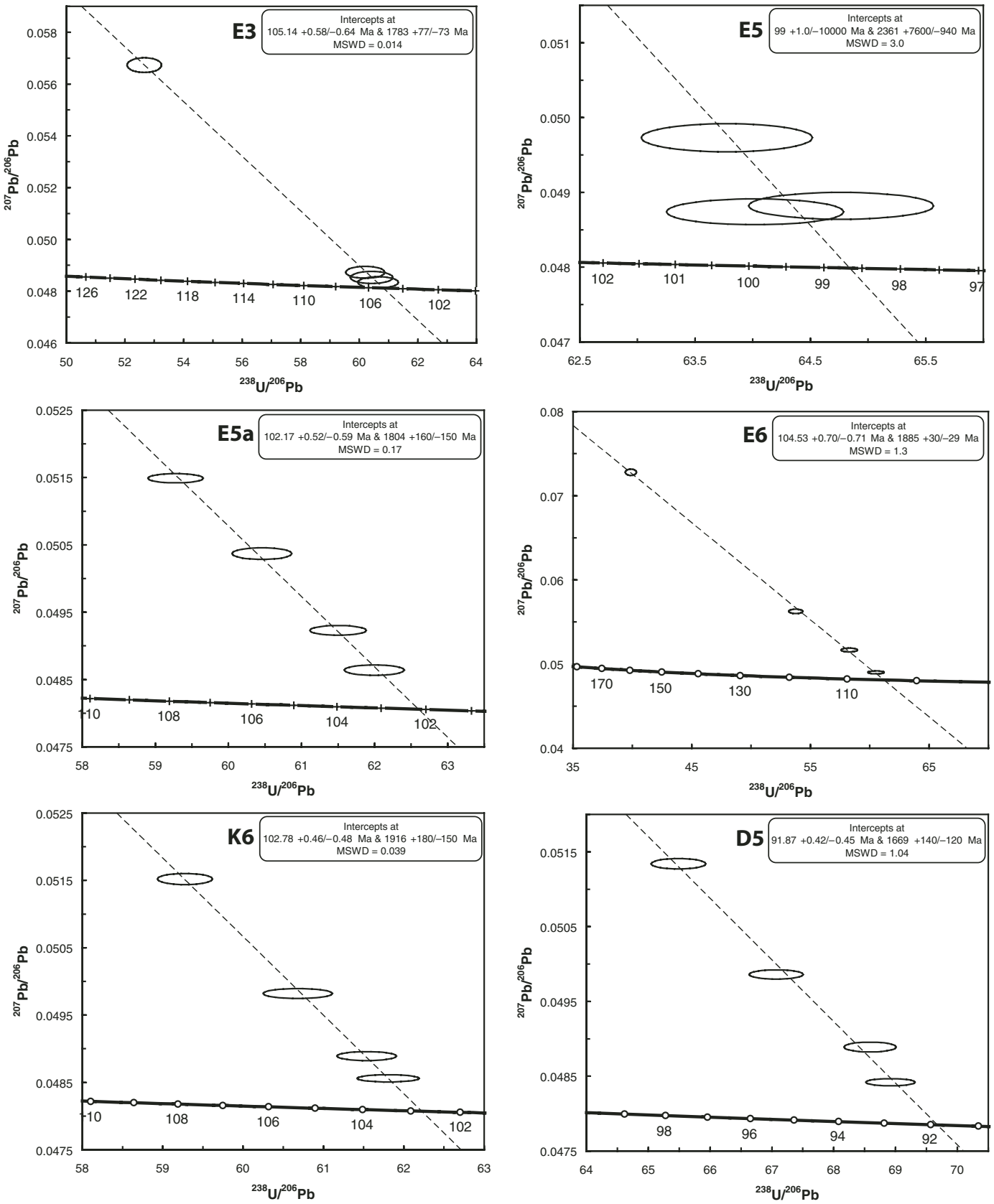

Figure 5. Concordia plots and solutions for discordant samples of Erskine Canyon sequence, Kern River, and Domelands intrusive suites (after Ludwig, 2001). MSWD—mean square of weighted deviates.

These data were from single-collector TIMS analyses, and thus their precision is notably low relative to most of the data presented here (Table DR1 [see footnote 1]; Figs. 4 and 5 [concordia plots]). Some of these samples, as well as additional samples from the sequence, have been analyzed by higher-precision multicollector techniques. We present the entire data set on the sequence, including analyses from both techniques. Data are presented for two hypabyssal intrusions and two ash-flow tuffs from the Erskine Canyon section (samples E1–4, Fig. 3), one ash-flow tuff from Piute Lookout (E5), a sample from the Yellowjacket Ridge volcanic neck (E6), and a sample from a vestigial block within high-strain tectonites of the proto–Kern Canyon fault (E7). Sample E1 is from a rhyolitic intrusive complex within mainly marble of the Kings sequence basement lying beneath the Erskine Canyon section. It yields an externally concordant age of 104.5 ± 0.4 Ma (Fig. 4). Sample E2 is from a pepperitic rhyolitic sill that was emplaced into quartzite-clast talus under subaqueous conditions. Its relatively low-precision data points are in near external concordance, but they are displaced slightly above concordia (Fig. 4). Such displacement off concordia is interpreted to reflect minor entrainment of zircon from the hosting detrital zircon-rich sediment. Contact metamorphism of the Erskine Canyon intact section was in low- to subhornblende hornfels facies, and the general coincidence of the E2 data array with other, higher-precision data argues against a disturbance mechanism for the discordance. Furthermore, the plutons that impart the contact aureole are, as discussed in the following, part of the subvolcanic intrusive complex for the Erskine Canyon sequence. We thus adopt an entrainment mechanism for the minor discordance, leading to an interpreted emplacement age of 105.4 ± 1.0 Ma for the sill. Continuing up-section, the E3 ash flow yields generally discordant ages, but its fine fraction is marginally concordant. Its three finer fractions mimic the E2 data, but its coarsest fraction is dispersed significantly off of concordia, indicating a substantial i/e component of Proterozoic zircon (Fig. 5). The E3 array defines a lower intercept of 105.1 ± 0.6 Ma and an upper intercept of 1783 ± 80 Ma. The lower intercept is interpreted as the eruption age, and the upper intercept is interpreted as the average age of the i/e zircon component. Sample E4 is another ash-flow unit that is ~100 m up-section from sample E3. It yields an externally concordant age of 104.0 ± 0.3 Ma (Fig. 4).

A preliminary U/Pb zircon age of 98 ± 3 Ma was reported for the sample E5 ignimbrite (Saleeby and Busby-Spera, 1986). These were low-precision single-collector TIMS data, and, furthermore, the rock unit is a relatively high-grade metamorphic tectonite within the proto–Kern Canyon fault. Accordingly, we resampled the body, abraded the zircon to a well-rounded state, to minimize grain boundary disturbance effects (after Krogh, 1982), and reanalyzed multiple fractions using higher-precision multicollector TIMS techniques. As with the original data, the E5 zircon shows a discordance pattern characteristic of the i/e component of Proterozoic zircon. The new data (E5a on Fig. 5) show a distinct upward shift of the $^{206}Pb/^{238}U$ ages relative to the original ages (E5 on Fig. 5), but there is a steeply inclined dispersion of $^{207}Pb/^{206}Pb$ ages similar to that of the original data. These topologic relations are interpreted to indicate that the discordance is dominated by the i/e mechanism and that during high-grade ductile deformation and metamorphism, which occurred within ~10 m.y. following eruption, the zircon grain margins were partially disturbed. The lower intercept of E5a (102.2 ± 0.5 Ma) is interpreted as an approximate eruption age, and the upper intercept of 1804 +160/–150 Ma is interpreted as the average age of the i/e zircon component.

Sample E6 is from a dacite porphyry phase of the Yellowjacket Ridge volcanic neck. It too shows a discordance array that is typical of the i/e component of Proterozoic zircon (Fig. 5). The lower intercept of 104.5 ± 0.7 Ma is interpreted as the emplacement/eruption age, and the upper intercept of 1885 ± 28 Ma is interpreted as the average age of the i/e zircon component. The lower-intercept age is indistinguishable from the ages determined for the ignimbrites and hypabyssal rocks of Erskine Canyon, supporting the interpretation that the Yellowjacket Ridge body is a part of the Erskine Canyon sequence that has been offset in a dextral sense by the Kern Canyon fault. Sample E7 is an ~20-m-scale vestigial lens rhyolitic rock encased in highly phyllonitic metavolcanics of the proto–Kern Canyon fault in the north shore area of Lake Isabella. This sample yielded a meager zircon population that yielded a U/Pb age spectrum with an apparent age of 106.5 ± 3.4 Ma (Fig. 6). The spread in the ages is permissive of either minor disturbance of some grains and/or a minor i/e component in other grains. We provisionally interpret the age of sample E7 as ca. 105 Ma.

The zircon age data for samples E1–E4 reveal a pronounced phase of silicic ignimbrite activity at 104–105 Ma, the products of which were ponded against a high-relief fault scarp within a subaqueous depression. The scarp faced inward to a depression, which perhaps coincided with the early trace of the proto–Kern Canyon fault, but subsequent deformation along the shear zone has obliterated the details of its proximal to distal stratigraphic and structural relations (Fig. 3, cross section). The ca. 102 Ma age from the E5 ignimbrite presents the possibility that volcanic ponding persisted for ~2–3 m.y. along the zone, but the sample E5a lower-intercept age could encompass a minor disturbance component, resulting in an erroneous expansion of this time interval.

Stratigraphic relations of the Erskine Canyon sequence are important for constraining the depth interval over which the coeval Kern River intrusive suite was emplaced (Fig. 3). The minimum stratigraphic thickness of the volcanic section is ~1.3 km, and an additional ~0.6 km of hypabyssal intrusives lie between the base of the section and subvolcanic plutons of the Kern River suite. Map relations between Erskine and Bodfish Canyons further indicate that the Kbo unit of the Kern River suite was emplaced up into the interval that contained distinctly hypabyssal textured intrusives. The Kbo unit could represent a "stubby" sill or laccolith complex that developed beneath the volcanic depression. To the north, the Yellowjacket Ridge volcanic neck is cut out along its western margin by the Kkr unit of the Kern River suite (Fig. 2),

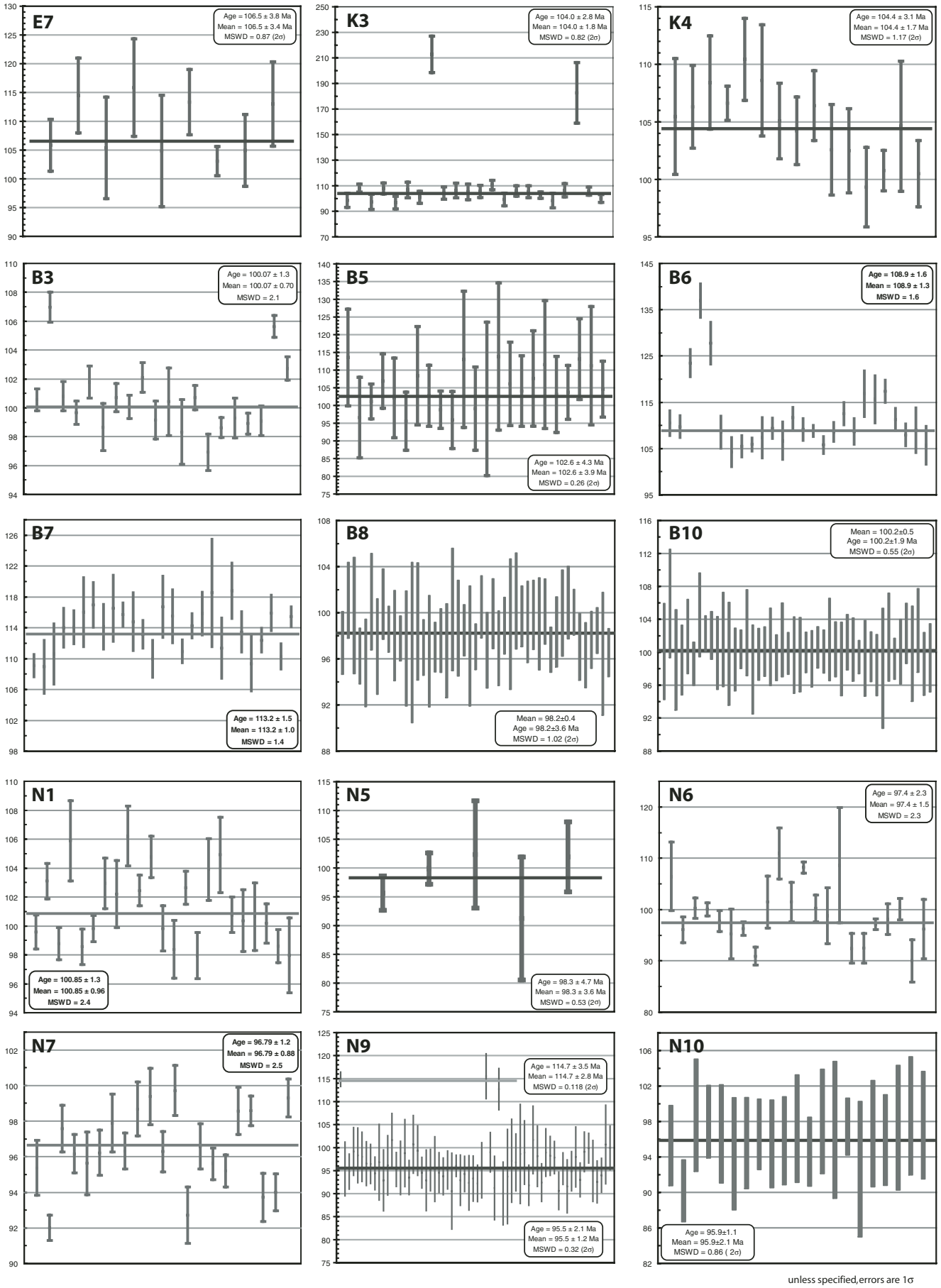

unless specified, errors are 1σ

Figure 6. U/Pb age-frequency spectra from laser-ablation–inductively coupled plasma–mass spectrometry (ICP-MS) data on the Erskine Canyon sequence, and the Kern River, Bear Valley, and Needles intrusive suites (after Ludwig, 2001). Vertical axes of each frame are in Ma. MSWD—mean square of weighted deviates.

suggesting that plutons of the suite in this area were intruded at even shallower levels than the base of the volcanic-hypabyssal section in Erskine Canyon.

Kern River Intrusive Suite

Intrusive units of this suite for which U/Pb zircon age data are presented include the granite of Kern River (Kkr), granite of Portuguese Pass (Kpp), granite of Bodfish Canyon (Kbo), granite of Baker Point (Kbp), and commingled mafic intrusives within the granite of Saddle Springs Road (Kss). The latter unit appears to be a complex of mafic variably textured intrusives that were commingled with granitic rocks of Bodfish Canyon affinity. The Kern River and Baker Point units in particular have characteristics of shallow-level igneous emplacement, including porphyritic phases with fine-to-aphanitic groundmass textures, and sharp discordant contacts, internal, with one another, and with hypabyssal and pendant rocks. Such features along with the age data presented herein and structural-stratigraphic relations indicate that plutons of this suite were the epizonal roots of the Erskine Canyon volcanic complex.

The granite of Kern River is the most voluminous pluton of this suite. It is a composite body with both subtle and sharp internal contacts marked by textural variations and locally accented by commingled mafic dikes and inclusion clusters. It is cut internally by a series of hypabyssal-textured dikes named the granite of Baker Point (Ross, 1995). Along its eastern to northern margins, the Kern River granite cuts sharply across structures within the bounding Fairview pendant. North of the Yellowjacket Ridge volcanic neck, its commingled marginal zone extends in a shallow east-dipping sill-like fashion into the bounding pendant as though it were "stacked-in" beneath the Yellowjacket Ridge body. In the Erskine Canyon area, lenticular apophysies of both Kern River and Bodfish Canyon granite extend concordantly into the Kings sequence–Erskine Canyon sequence section as very thick sill-like bodies (Fig. 3). We present new zircon age data for four phases of the Kern River granite (samples K1–K4). As shown on Figure 2, the granite has been offset along the Kern Canyon fault. Samples K1 and K2 are from west of the fault. They yield externally concordant ages of 105.0 ± 0.3 Ma and 104.3 ± 0.5 Ma, respectively (Fig. 4). Samples K3 and K4 are from east of the Kern Canyon fault. They yield U/Pb age-frequency spectra that indicate ages of 104.0 ± 1.8 Ma and 104.4 ± 1.7 Ma, respectively (Fig. 6). Some discordant zircon grains from sample K3 clearly

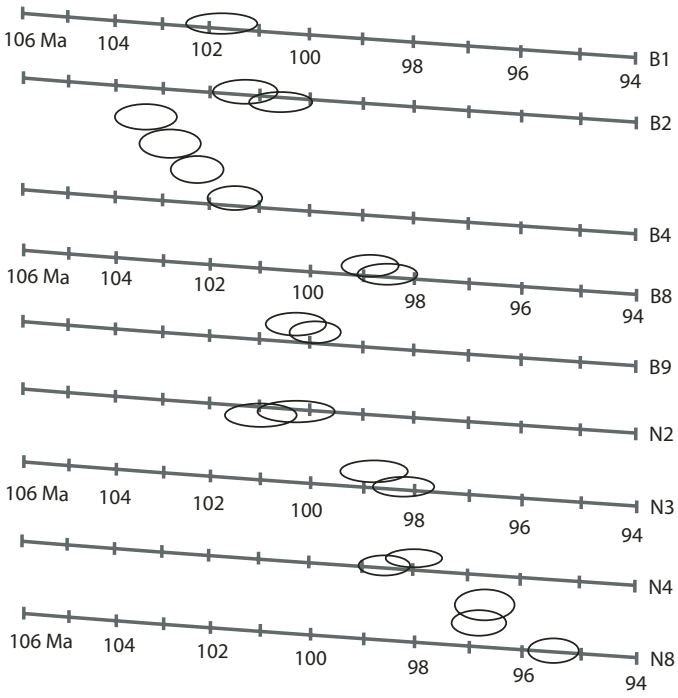

Figure 7. Concordia line segments (after Tera and Wasserburg, 1972) stacked in $^{207}Pb/^{206}Pb$ space for concordant or near-concordant data error ellipses for samples from the Bear Valley and Needles intrusive suites. Errors are 2σ; plotting procedure is modified from Ludwig (2001).

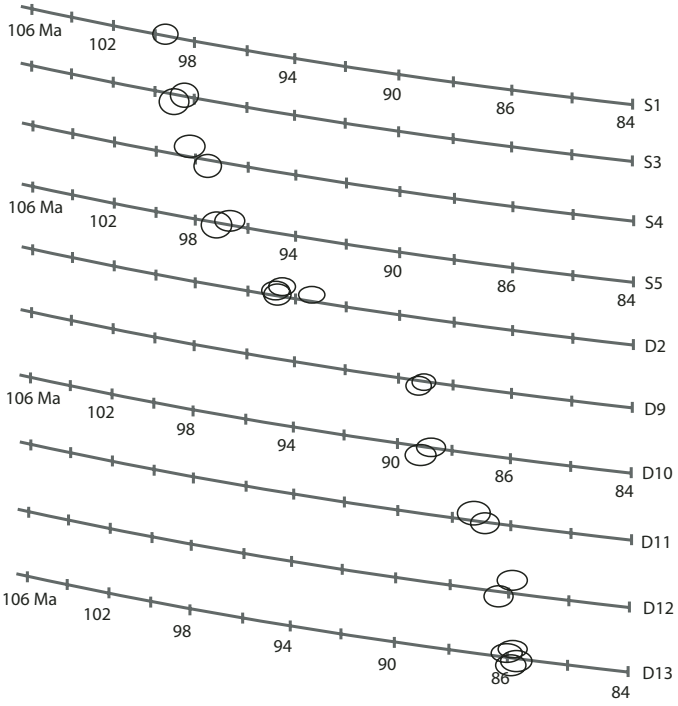

Figure 8. Concordia line segments (after Tera and Wasserburg, 1972) stacked in $^{207}Pb/^{206}Pb$ space for concordant or near-concordant data error ellipses for samples from the South Fork and Domelands intrusive suites. Errors are 2σ; plotting procedure is modified from Ludwig (2001).

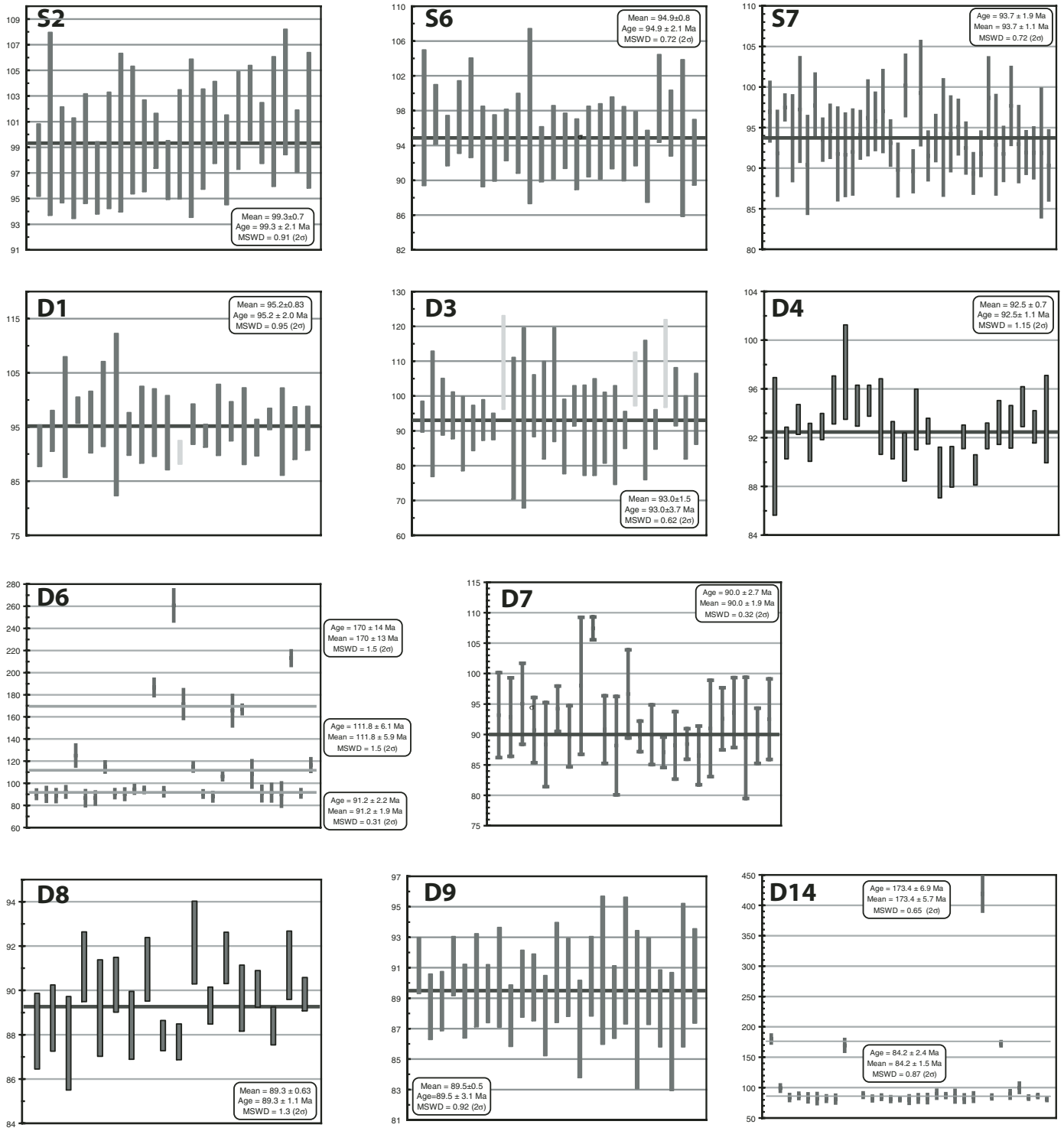

Figure 9. U/Pb age-frequency spectra from laser-ablation–inductively coupled plasma–mass spectrometry (ICP-MS) data on the South Fork and Domelands intrusive suites (after Ludwig, 2001). Vertical axes of each frame are in Ma. MSWD—mean square of weighted deviates.

show i/e components, and some of the scatter of the K4 data could arise from similar, but minor i/e components.

Additional distinctively leucocratic plutons of the Kern River suite include the granite of Portuguese Pass (sample K5) and the granite of Bodfish Canyon (K6). Both of these plutons are compositionally similar to the Kern River granite, but they typically lack the distinctive porphyritic textures of the latter. The Portuguese Pass pluton is separated from the granite of Kern River by a narrow pendant and is otherwise surrounded by northernmost Bear Valley and Needles suite plutons (Fig. 2). The Bodfish Canyon pluton is encased in Erskine Canyon hypabyssal rocks and pendant rocks except to the south, where it grades into the granite of Saddle Springs Road. Sample K5 from the Portuguese Pass unit yielded a sparse fine-grained zircon population, which gave an internally concordant age of 103.2 ± 0.8 Ma (Fig. 4). Sample K6 from the Bodfish Canyon unit yielded a discordant array of fractions dispersing upward from a lower intercept of 102.8 ± 0.5 Ma, and projecting to an upper intercept of 1916 +1180/–150 Ma (Fig. 5). The lower intercept is interpreted as the igneous age, and the upper intercept is interpreted as the average age of the i/e component.

A sample of commingled dioritic dike rock in the granite of Saddle Springs Road (sample K7) yielded a slightly discordant age array (Fig. 4). Its fine fraction yielded a nearly internal concordant age, while its coarser two fractions were displaced slightly more off of concordia. The dispersion pattern off of concordia is suggestive of a minor i/e component of substantially older, Proterozoic (?) zircon. The 102.5 ± 0.5 Ma age of the nearly concordant fraction is interpreted as the igneous age of the commingled mafic rock, which is consistent with the 102.8 ± 0.5 Ma age determined for the Bodfish Canyon granite, with which it is commingled.

The largest known texturally homogeneous body from the Baker Point "granite" composite dike unit was sampled adjacent to where it is observed to intrude the Kern River granite (sample K8). The rock in this location is a dacite porphyry. It yielded an externally concordant age of 102.6 ± 0.5 Ma (Fig. 4). The texture of this sample is transitional between the distinctly porphyritic-fine groundmass phases of the Kern River granite and textures observed in the Erskine Canyon sequence hypabyssal intrusions. The Baker Point dikes are interpreted as being consanguineous with the hypabyssal intrusions.

In summary, samples studied from Kern River intrusive suite cluster between 105 and 102 Ma in age, like those of the Erskine Canyon sequence. Initial strontium isotopic data presented in Kistler and Ross (1990) support the petrogenetic affinity of the Erskine Canyon sequence and the Kern River intrusive suite, the values of which overlap and are distinct from all other values presented for rocks west of the proto–Kern Canyon fault. These relations in conjunction with structural position and textural relations indicate that the Kern River suite is part of the epizonal plutonic complex of the Erskine Canyon sequence. Cross-sectional relations suggest that the Bodfish Canyon granite was emplaced over a depth interval of ~2–4.5 km (Fig. 3). If the eastern limit of the overlying Erskine Canyon sequence in the Figure 3 map area approximates the top of the volcanic section, and if bulk shortening strain in that part of the section deformed within the proto–Kern Canyon fault may be approximated as 0.5 (Nadin and Saleeby, this volume), then the Bodfish Canyon granite is further constrained to have been emplaced within a depth interval of ~3.5–6 km. Structural and age relations at the southern end of the Kern River granite suggest even a shallower level of emplacement (Fig. 3), and as discussed already, relations between the northern Kern River granite and the Yellowjacket Ridge volcanic neck suggest a similar shallow level of emplacement.

Bear Valley Intrusive Suite

The Bear Valley suite was originally defined as a suite of gabbroic to tonalitic intrusives of 102–98 Ma age within the Tehachapi complex, and it was later extended to include intrusives as old as 105 Ma further to the west in the western Tehachapi Range (Saleeby et al., 1987; Pickett and Saleeby, 1994). Regional mapping extends the principal plutonic units of this suite northward to ~35.75°N (Ross, 1989, 1995; this study). The principal units that extend northward into the study area are the tonalite of Bear Valley Springs (Kbv) and the tonalite of Mount Adelaide (Kma) (Fig. 2). Based on petrographic similarities, continuity in compositional variations, structural position, age relations, and Sr_i, the granodiorite of Poso Flat (Kpf) is included in the Bear Valley suite. The Poso Flat unit mesoscopically resembles parts of the tonalite of Bear Valley Springs, although its K-feldspar modes place it marginally within the granodiorite field, and it is much more homogeneous. The Poso Flat unit is considered the northern, relatively shallow-level terminus of the Bear Valley suite, although there are small screens of the Bear Valley Springs unit north of the Poso Flat unit between Needles and Kern River suite rocks.

New U/Pb zircon age data on the Bear Valley suite are presented here for a commingled mafic intrusive body within the Bear Valley Springs unit (B1), four samples of the Bear Valley Springs tonalite (B2–B5), the type location of the Mount Adelaide unit at Mount Adelaide (B8), and two samples from the Poso Flat unit (B9 and B10). Also, two 100-m-scale enclaves of Early Cretaceous tonalite, not readily distinguishable in the field from much of the Bear Valley Springs unit, were dated (B6 and B7). Early Cretaceous tonalite and tonalite gneiss enclaves are common within the deeper-level exposures of the Bear Valley Springs unit, and they may be more common throughout the region than what is readily recognized.

Sample B1 is from an ~2 km × ~4 km diorite enclave that is partly commingled with, and lies concordantly within, foliated Bear Valley Springs tonalite. Such mafic members of the suite range up to ~5 km in diameter and down to meter-scale disrupted dike and inclusion swarms. Some of the larger bodies range in composition from hornblende diorite to hornblende (±pyroxenes and rare olivine) gabbros and melagabbros. Sample B1 yielded one sparse fine fraction, which gave an internally concordant age of 101.8 ± 0.4 Ma (Fig. 7). The proximal Bear Valley Springs host for the diorite is typical of much of the tonalite: it is steeply

foliated and rich in deformed mafic inclusions. Within ~3 km of the diorite enclave, however, there is a nonfoliated, inclusion-poor zone of the tonalite that cuts foliated inclusion-rich tonalite. Sample B2 from this more homogeneous zone yielded an externally concordant age of 101.0 ± 0.3 Ma (Fig. 7). The sample B1 and B2 data along with the intrusive relations bracket the foliated inclusion-rich tonalite to ca. 101.5 Ma in this area.

Samples B3 and B4 are from the Bear Valley Springs unit in the Walker Basin area (Fig. 2). These samples are from foliated, mafic inclusion-rich tonalite typical of the Bear Valley Springs unit. Sample B3 yielded a U/Pb age spectrum that indicates a 100.1 ± 0.7 Ma age (Fig. 6). The age spectrum includes discordant grains indicative of a minor i/e component. Sample B4 yielded a fine internally concordant fraction and coarser slightly discordant fractions that disperse off of concordia progressively with grain size (Fig. 7). Such dispersion is suggestive of very a minor i/e component of older (Proterozoic?) grains, but to such a limited extent that a concordia intercept solution carries little meaning. The internally concordant age of 101.5 ± 0.4 Ma is interpreted as an approximate igneous age. Small screens of the Bear Valley Springs tonalite that are locally rich in commingled gabbros lie between Needles suite plutons and older pendant and Kern River suite rocks at ~35.75°N. Sample B5 is from the western screen. It yields U/Pb age spectra suggestive of an igneous age of 102.6 ± 3.9 Ma (Fig. 6). These small screens constitute the only known locations where the tonalite is in contact with older Kern River suite rocks. The eastern screen possesses local sill-like structures, which include commingled gabbros, suggesting that it was stacked in beneath pendant and Kern River suite rocks.

Structural and textural relations and age data resolve two significant screens of Early Cretaceous tonalite within the tonalite of Bear Valley Springs unit of the study area. In the Walker Basin area, an ~100-m-wide screen of foliated biotite tonalite occurs along the Bear Valley Springs northern contact with pendant rocks (Fig. 3). Sample B6 is from this screen. It yielded U/Pb age spectra that indicate an age of 108.9 ± 1.3 Ma (Fig. 6). The age spectra include discordant grains indicative of a minor to modest i/e component of older zircon. An additional enclave of Early Cretaceous tonalite was discovered ~6 km west of the sample B6 enclave, across the Kern Canyon fault (Fig. 2). This enclave is ~500 m in scale, although poor exposure quality limits the resolution of its detailed map pattern. Sample B7 is from this enclave. It yields U/Pb age spectra that indicate an age of 113.2 ± 1.0 Ma. The scatter in the data points of this spectrum permits the possibility of both minor i/e components in some grains, and minor disturbance in other grains.

The Mount Adelaide and Poso Flat units of the Bear Valley suite are much more homogeneous than the Bear Valley Springs unit, and they typically lack the synplutonic deformation fabric of the latter. Sample B8 is from the Mount Adelaide unit at its type location near the western edge of the Sierra (Fig. 3). It yielded an externally concordant age of 98.6 ± 0.6 Ma (Fig. 7). A duplicate split of this sample yielded U/Pb age spectra that indicate an age of 98.2 ± 0.4 Ma (Fig. 6), which shows agreement between the two analytical techniques within their respective uncertainties. An error weighted mean, between the two techniques, of 98.4 ± 0.2 Ma is adopted for this sample. This matches the youngest age determined for the Bear Valley suite, which was determined on the Bear Valley Springs tonalite within the deep-level exposures of the Tehachapi complex (Saleeby et al., 1987). The Mount Adelaide unit of the sample B8 area is observed cross-cutting the adjacent Bear Valley Springs unit as well as its synplutonic deformation fabric, consistent with the age data.

Samples B9 and B10 were taken from the Poso Flat unit. Sample B9 yielded an externally concordant age of 100.1 ± 0.3 Ma (Fig. 7). Sample B10 yielded U/Pb age spectra that indicate an age of 100.2 ± 0.5 Ma (Fig. 6). These ages are in excellent agreement with one another, and they are consistent with the observation that the Poso Flat unit is uniquely homogeneous relative to most rocks of the Bear Valley suite.

In summary, the zircon age data for the relatively shallow-level exposures of the Bear Valley intrusive suite in the study area indicate a clustering of igneous ages for the tonalite of Bear Valley Springs, including commingled mafic intrusives, and the Mount Adelaide and Poso Flat units, which are all within 98–102 Ma. This is similar to the age range that was determined for much of the suite in the Tehachapi complex to the south, and, together, these data sets indicate that most of the Bear Valley suite was assembled over the same time interval along its entire ~100 km north-south extent. The Bear Valley Springs unit is characterized by a myriad of compositionally similar small intrusions, which typically display steeply dipping synplutonic deformation fabrics accentuated by the remnants of deformed commingled mafic dikes. The various members of the Bear Valley Springs unit also display a wide range of Sr_i values (0.70424–0.70601), and values reach as high as 0.70677 adjacent to migmatitic metasedimentary enclaves (Saleeby et al., 1987; Kistler and Ross, 1990; Pickett and Saleeby, 1994). In contrast, the Mount Adelaide and Poso Flat units are more homogeneous at outcrop and map scale, possess a much more restricted range of Sr_i (0.70427–0.70503), and appear to have been emplaced over the more restricted time interval of ca. 100–98 Ma. Furthermore, the Mount Adelaide and Poso Flat units are restricted to exposure levels of ≤4 kbar, whereas the Bear Valley Springs unit extends from ~8 kbar to perhaps as shallow as ~2 kbar in the north where it intrudes rocks of the Kern River suite (Ague and Brimhall, 1988; Pickett and Saleeby, 1993; Nadin and Saleeby, this volume).

Needles Intrusive Suite

The northern end of the Bear Valley intrusive suite is cut by the southern end of a belt of mainly granodioritic to locally tonalitic plutons, which we refer to here as the Needles suite. Some of the Needles suite plutons resemble in mesoscopic structure and texture some phases of the Bear Valley Springs unit as well as the more uniform Mount Adelaide and Poso Flat units (Ross, 1989). The Needles suite plutons occur as smaller, more orderly nested bodies, as compared to the principal units of the Bear

Valley suite. This distinctive belt of plutons continues northwestward beyond the limits of the study area (du Bray and Dellinger, 1981). The Needles suite plutons may also be contrasted from the Bear Valley suite by their higher and more restricted range of Sr_i (0.70616–0.70669, with outliers as high as 0.70742), and a younger age range of emplacement (ca. 95–101 Ma).

Principal plutons of the Needles suite for which new zircon age data are presented include: the granodiorite of Alder Creek (Kal), the granodiorite of Brush Creek (Kbc), the tonalite of Dunlap Meadow (Kdm), the granodiorite of Pine Flat (Kpi), the granodiorite of Alta Sierra (Kas), the granodiorite of Peppermint Meadow (Kpm), the granodiorite of the Needles (Kne), and the granodiorite of Wagy Flat (Kwf) (Fig. 2; Table 1). The Alder Creek unit appears to be the oldest dated pluton of the suite. Textural and structural variations of this unit indicate that it is a composite body. Sample N1 is from the most homogeneous and aerially extensive zone of the pluton. It yielded U/Pb age spectra that indicate an age of 100.9 ± 1.0 Ma (Fig. 6). The spread of data in the N1 spectra presents the possibility that there is a minor i/e component in the system, which could skew the mean age to the high side. This leaves open the possibility that the Alder Creek body is younger (ca. 98–100 Ma) than the mean age given. The granodiorite of Brush Creek is a distinct member of the Needles suite in that it is notably melancratic, enriched in mafic enclaves, and is relatively old as compared to most other plutons of the suite. It may in fact be older than the Alder Creek unit. In a number of aspects, it strongly resembles the Kri unit and felsic portions of the Kcf unit of the South Fork suite. As such, it may be part of an equivalent intrusive complex, offset by the proto–Kern Canyon fault (Nadin and Saleeby, this volume). The Brush Creek body is nested in along the marginal zone of the much larger Peppermint Meadows pluton, against the Fairview pendant (Fig. 2). Sample N2 from the Brush Creek body yielded an externally concordant age of 100.6 ± 0.4 Ma (Fig. 7). This age matches the older ages for the Kri and Kcf units of the South Fork suite, discussed later.

Samples N3 and N4 are from the tonalite of Dunlap Meadow and the granodiorite of Pine Flat, respectively. Map relations of these two bodies suggest that they are part of a concentrically zoned pluton, where the more felsic phases are in the interior (Fig. 2). Sample N3 yielded an externally concordant age of 98.5 ± 0.5 Ma, and sample N4 yielded an externally concordant age of 98.3 ± 0.4 Ma (Fig. 7).

The northernmost plutons studied here from the Needles suite consist of the granodioritic plutons of Peppermint Meadows and the Needles (Fig. 2). Textural variations, and local internal contacts within and between these bodies, suggest that they are each composites of several compositionally and texturally overall similar intrusive sequences. Samples N6 from the Peppermint Meadows pluton, and N7 from the Needles pluton yielded similar U/Pb age spectra with considerable scatter about the mean. The N6 spectra suggest an age of 97.4 ± 1.5 Ma, and the N7 spectra suggest an age of 96.8 ± 0.9 Ma (Fig. 6). Sample N7 is on the margin of the proto–Kern Canyon fault, and it exhibits a modest ductile deformation fabric. Part of its age scatter could be due to minor disturbance of its more labile grains. Sample N8 is from the interior of the Needles pluton. It is from ~5 km west of the proto–Kern Canyon fault, and it has a pristine igneous texture. It yielded an array of internally concordant to slightly discordant fractions that suggest an age of 96.0 ± 0.5 Ma, with a very minor i/e component (Fig. 7). Such a minor i/e component is further suggested in the scatter of the U/Pb age spectra of samples N6 and N7 (Fig. 6). Unfortunately, the resolution of $^{207}Pb/^{206}Pb$ ages by the laser-ablation ICP-MS technique is too low to better resolve the hypothetical i/e component. The convergence of the N6, N7, and N8 ages, however, strongly suggests that the Peppermint Meadows–Needles composite of texturally and compositionally similar plutons is ca. 96 Ma in age.

The southeastern end of the Needles suite consists of the texturally and structurally distinct granodiorites of Alta Sierra and Wagy Flat. These are relatively uniformly NW-striking elongate plutons that are both offset 12 ± 1 km dextrally by the Kern Canyon fault (Nadin and Saleeby, this volume) (Fig. 2). They cut the northeastern end of the Bear Valley suite, and, along with the Alder Creek body, they have calved off a screen(s) of marginal phase gabbros and tonalites of the Bear Valley suite and their host pendant rocks. Sample N5 is from the Alta Sierra pluton, and it yielded a meager zircon population with U/Pb age spectra that suggest an igneous age of 98.3 ± 3.6 Ma (Fig. 6). Samples N9 and N10 are from the Wagy Flat pluton, on opposite sides of the Kern Canyon fault (Fig. 2). Sample N9 to the west of the Kern Canyon fault yielded a U/Pb age spectra that suggest an igneous age of 95.5 ± 1.2 Ma (Fig. 6). The three discordant data grains are clearly the products of i/e; the source in this case appears to have been Early Cretaceous plutonic rocks akin to those that occur as enclaves within the Bear Valley suite. Sample N10 to the east of the Kern Canyon fault yielded U/Pb age spectra that suggest an age of 95.9 ± 2.1 Ma (Fig. 6). The granodiorite of Wagy Flat appears to be the youngest member of the Needles suite, although it could be the same age as the Peppermint Meadows–Needles complex.

In summary, the apparent age range of the Needles intrusive suite is 95–101 Ma. This age range is clearly offset from the ca. 98–102 Ma range of the Bear Valley suite. Clear contrasts between these two suites are also exhibited by the more uniform and overall more felsic composition of the Needles suite, and by its consistently higher Sr_i values (Table 1). As discussed further later, the Needles suite Sr_i values are not only notably more radiogenic, but their overall systematics are more orderly. Multiple samples from individual units form strong linear arrays on Rb/Sr evolution diagrams, and a number of units share the same arrays (Kistler and Ross, 1990). Isochron ages derived from these arrays agree, within uncertainty, with the zircon ages as well. In contrast, a large sample set from the various intrusive units of the Bear Valley suite shows little or no systematics and a wide range of Sr_i (Saleeby et al., 1987; Pickett and Saleeby, 1994; Kistler and Ross, 1990). These relations suggest a greater degree of homogenization in the source region for the Needles suite magmas, and little or no contamination upon ascent.

South Fork Intrusive Suite

The South Fork intrusive suite is named for a relatively small cluster of ca. 94–100 Ma plutons composed of leucogranite, mafic granodiorite, diorite, and gabbro that spans the South Fork Valley of the Kern River (Fig. 2). This suite is unique to the study area by the degree of deformation and metamorphism that its wallrock pendants experienced during its intrusion. This included the development of pervasive high-strain metamorphic tectonites and extensive migmatization of psammite-pelite units along relatively broad contact aureoles (Saleeby and Busby-Spera, 1986; Zeng et al., 2005). This suite is also distinct by its wide range of Sr_i values (0.70593–0.73500), as well as the presence of marginal zones in some plutons that exhibit severe zircon entrainment by the intermixing of melt products from adjacent migmatitic pendant rocks (Saleeby and Busby-Spera, 1986; Kistler and Ross, 1990; Zeng et al., 2005). We present new U/Pb zircon age data on the three most aerially extensive plutons of the South Fork suite, which are the quartz diorite of Cyrus Flat (Kcf), the alaskite of Sherman Pass (Ksp), and the granodiorite of Rabbit Island (Kri) (Fig. 2).

The quartz diorite of Cyrus Flat consists of a hornblende-rich gabbroic zone that is concentrated along its current west-central map area where it is truncated by the proto–Kern Canyon fault. This mafic zone is mantled to the north, east, and south by intergradational rocks ranging from quartz diorite to mafic granodiorite. The western margin of the pluton is ductilely sheared by the proto–Kern Canyon fault and intruded by the Cannell Creek granite of the Domelands suite. The eastern margin of the Cyrus Flat pluton is interleaved with the granodiorite of Rabbit Island as well as a series of leucogranite dikes. Prior to truncation by the proto–Kern Canyon fault and intrusion of the Cannell Creek pluton, the Cyrus Flat body may have formed a concentrically zoned pluton, or ring dike complex, akin to a number of other relatively small mafic plutons that have been studied in detail in the southern Sierra Nevada batholith (Mack et al., 1979; Clemens-Knott and Saleeby, 1999). We present new U/Pb zircon data for a hornblende-hypersthene leucogabbro from the western core zone of the Cyrus Flat pluton (sample S1). Its meager fine zircon yielded an internally concordant age of 99.6 ± 0.3 Ma (Fig. 8). Zircon populations for several samples of the more felsic zones of the pluton are so severely contaminated with Proterozoic zircon that they carry little igneous age information.

The principal felsic units of the South Fork suite are dispersed along a NW-trending belt, partly within the eastern margin of the proto–Kern Canyon fault, but to a greater extent encased as a series of enclaves within Domelands suite granitoids (Fig. 2). These consist of the alaskite of Sherman Pass and the granodiorite of Rabbit Island (Fig. 2). Sample S2 is from the elongate alaskite pluton, near its northern terminus. This sample yielded U/Pb age spectra that suggest an igneous age of 99.3 ± 0.7 Ma (Fig. 9). Alaskitic (leucogranite) dikes are locally commingled with the Cyrus Flat mafic pluton, and the correspondence of the S1 and S2 ages, within uncertainty, further suggests that the Sherman Pass and Cyrus Flat plutons were at least in part comagmatic. The granodiorite of Rabbit Island is a composite body consisting of mafic granodiorites, and microdiorite as coherent and commingled dikes and inclusion swarms. The mafic granodiorites were emplaced over an apparent 5 m.y. time interval coincident with other small South Fork suite plutons to the southwest, which are shown on Figures 2 and 3 as the granodiorite of Goat Ranch Canyon (Kgr) and nondifferentiated South Fork suite (Zeng and Saleeby, 2005, written commun.). Sample S3 is from the most homogeneous and aerially extensive phase of the Rabbit Island pluton; it yielded an externally concordant zircon age of 99.0 ± 0.4 Ma (Fig. 8). This relatively homogeneous phase of the pluton extends southeastward across the South Fork Valley as a lobe-like feature within Domelands suite granitoids. Sample S4 is from the southern part of the relatively homogeneous zone of Rabbit Island granodiorite (Fig. 2). It yielded a marginally externally concordant age of 97.8 ± 0.7 Ma (Fig. 8). The northern tip of the contiguous Rabbit Island pluton is attenuated along the eastern margin of the proto–Kern Canyon fault. Sample S5 is from ductilely deformed mafic granodiorite of this zone. It yielded an externally concordant age of 97.0 ± 0.4 Ma (Fig. 8). Younger phases of the Rabbit Island composite body are petrographically similar to the principal older phases discussed already, although they are typically poorer in commingled mafic dikes and inclusion swarms, and, in the southeast, they are extensively cut by felsic dikes. Sample S6 is from such a younger phase, at the southern end of the pluton. It yielded U/Pb age spectra that suggest an igneous age of 94.9 ± 0.8 Ma (Fig. 9). Sample S7 is from a younger phase of the pluton to the north (Fig. 2). This sample yielded U/Pb age spectra that suggest an igneous age of 93.7 ± 1.1 Ma. At this location, spaced high-temperature ductile shears of the marginal zones of the proto–Kern Canyon fault are common. The scatter of the data points for this sample permits the possibility of minor disturbance during high-temperature shearing, or emplacement of the voluminous Domelands suite to the east. For this reason, we adopt a ca. 94 Ma age for this youngest phase of the Rabbit Island unit.

In summary, the zircon age data suggest that the South Fork intrusive suite was emplaced over the 100–94 Ma time interval. It was emplaced under deeper-level and higher-strain conditions than the roughly coeval Needles suite to the west (Nadin and Saleeby, this volume; Zeng et al., 2005). As discussed next, Domelands suite intrusive activity began at least locally as South Fork intrusive waned. The South Fork suite plutons were disrupted and deformed both by the proto–Kern Canyon fault to the west, and by the incremental emplacement of the younger Domelands suite to the east.

Domelands Intrusive Suite

The Domelands suite is the most extensive intrusive suite of the study area. It is restricted to the area east of the proto–Kern Canyon fault, and it constitutes one of the principal protolith

elements within the principal damage zone of the proto–Kern Canyon fault. This suite consists of three regionally extensive plutonic units, the granodiorite of Claraville, the granite of Castle Rock, and the Castle Rock granitic dike swarm(s). The Claraville unit is also referred to as the Whiterock (nonporphyritic) facies of the granite of Castle Rock (Ross, 1989, 1995). We retain the term Claraville, which was originally defined south of the study area where it has yielded U/Pb zircon dates around 91 ± 1 Ma (Saleeby et al., 1987; Wood and Saleeby, 2008). The Castle Rock unit is distinguished in this study by its pink K-feldspar megacrystic texture and common aplitic to pegmatitic granitic dikes. The Claraville locally contains pink K-feldspar phenocrysts that resemble those of the finer phenocrystic Castle Rock. The Castle Rock unit appears to be 1–3 m.y. younger than the Claraville unit. The Castle Rock granitic dike swarms consist of a myriad of tabular stocks, isolated and composite dikes, and interdike bridges, and within the proto–Kern Canyon fault, variably transposed dikes and completely transposed concordant sheets. The granite of Onyx, also grouped into the Domelands suite, appears to be principally dike rock as well, but it is distinctly older than the Castle Rock dikes. The Castle Rock granitic dike unit that is differentiated on Figure 2 is arbitrarily defined as the region where clearly resolvable felsic dikes constitute greater than 50% of the outcrop area. The Castle Rock dike unit contains screens of both Claraville and Castle Rock granitoids. Internal contact relations, textural variations, and the U/Pb age data indicate that much of the Castle Rock unit was constructed from numerous dikes and/or small tabular plutons. The Claraville unit possesses internal contacts as well, but its internal units appear to underlie larger map areas than those of the Castle rock unit.

The large-volume units of the Domelands suite were emplaced between 87 and 92 Ma. Some of the smaller units were emplaced between 93 and 95 Ma, thus overlapping with the youngest units of the South Fork suite. Domelands granitoids contrast sharply with the more mafic units of the South Fork suite, and they are different from the South Fork leucogranites because they have higher K-feldspar and biotite modes. Domelands suite rocks also show a much more restricted range of Sr_i values (0.70704–0.70930) than the 0.7093–0.7350 range exhibited by the South Fork suite (Kistler and Ross, 1990; Zeng et al., 2005).

The oldest units of the Domelands suite are the granite of Long Meadow, the granite of Cannell Creek, and the granite of Onyx. These lie in contrasting structural positions. The Long Meadow body is a large enclave within Castle Rock megacrystic granite. Sample D1 from the Long Meadow granite yielded U/Pb age spectra that suggest an igneous age of 95.2 ± 0.8 Ma (Fig. 9). The granite of Cannell Creek is a high-strain blastomylonite the lies concordantly within the proto–Kern Canyon fault. It runs for a strike distance of ~12 km within the shear zone, where, to the north, it interfingers with and is replaced by variably textured mylonitic Castle Rock granite, mainly dikes, informally named Goldledge granite by Busby-Spera and Saleeby (1990). Both the Cannell Creek and "Goldledge" granites bear critical structural and age relations that constrain the deformation history of the proto–Kern Canyon fault. These are discussed further later in the context of other Domelands suite age relations. Sample D2 is from the Cannell Creek unit. Three natural size fractions yielded two externally concordant ages of 94.7 ± 0.4 Ma, and an externally discordant yet internally concordant age of 93.4 ± 0.4 Ma on its fine fraction. One of the coarser fractions was abraded to a well-rounded state as a test to see if it had undergone grain-margin disturbance during high-temperature mylonitization. It yielded an internally concordant age of 94.8 ± 0.4 Ma, which is concordant with the two coarser fractions (Fig. 8). These data are interpreted to mark a 94.7 ± 0.4 Ma igneous age, where the finer fraction has undergone minor disturbance during high-temperature strain and annealing. The granite of Onyx consists primarily of fine-grained granitic dike rock. Sample D3 from the Onyx dikes yielded U/Pb age spectra that suggest an igneous age of 93.0 ± 1.5 Ma (Fig. 9). As discussed later, this is distinctly older than the widespread Castle Rock dikes. The only clearly resolvable host for the Onyx granite is the Rabbit Island granodiorite of the South Fork suite. The map relations of the South Fork and Domelands suites (Fig. 2) suggest that the Domelands suite grew from a core of Onyx and Long Meadow dikes and tabular plutons that initially intruded and dispersed South Fork suite host rocks.

Large-volume units of the Domelands suite consist of the Claraville and Castle Rock granites. Based on our age data and the textural criteria presented already, we extend the Claraville unit much further north than Ross (1995). Samples D4, D5, D6, and D7 are representative of large areas of the Claraville unit. Sample D4 yielded U/Pb age spectra that suggest an igneous age of 92.5 ± 0.7 Ma (Fig. 9). The scatter of the data presents the possibility of a very minor i/e component in many of the grains, which raises a concern that the filtered mean may be biased slightly to the high side. There is no reason to suspect that the Claraville unit of this region suffered any subsolidus disturbances. Sample D5 is from an equigranular phase of the Claraville that yielded a discordant array of data points with a 91.9 ± 0.4 Ma lower intercept and a 1669 +140/–120 Ma upper intercept (Fig. 5). The array is interpreted as an i/e trajectory, where the lower intercept approximates the igneous age and the upper intercept is an averaged age of the i/e component. Sample D6 yielded U/Pb age spectra that suggest an igneous age of 91.2 ± 1.9 Ma (Fig. 9). The discordant ages on the D6 spectra plot clearly reveal distinct i/e components. The groupings of a significant number of the aberrant points at ca. 111 Ma and 170 Ma strongly suggest the incorporation of older batholithic zircon. The two older ages of ca. 215 Ma and ca. 260 Ma could represent highly disturbed Proterozoic detrital grains from metaclastic pendant rocks or non- to little-disturbed batholithic zircon. Permian-Triassic as well as Jurassic batholithic units lie adjacent to the Claraville unit east of the Kern Plateau shear zone (Evernden and Kistler, 1970; Dunne and Saleeby, 1993). As discussed later, the aberrant ages of the D6 spectra are suggested to be a source inheritance feature. Sample D7 yielded U/Pb age spectra that suggest an igneous age of 90.0 ± 1.9 Ma.

Mafic granodiorites and tonalites occur locally within the Claraville unit. Some are commingled with the more felsic rocks, and some form homogeneous mappable bodies. Sample D8 is from the largest of such mafic bodies (Fig. 2). It yielded U/Pb age spectra that suggest an igneous age of 89.3 ± 0.6 Ma (Fig. 9). Relative intrusive relations between the D8 mafic body and the surrounding felsic granodiorite are ill defined and suggestive of comagmatic states. This suggests the possibility that Claraville felsic magmatism continued to ca. 89 Ma. Zircon age data presented already suggest that the Claraville unit was emplaced between ca. 92.5 and 89 Ma. This age range suggests that Claraville magmatism ceased as the megacrystic Castle Rock series of intrusions began their emplacement, as discussed later.

Samples D9, D10, and D11 are from relatively homogeneous areas of the Castle Rock granite. Sample D9 was analyzed by both techniques as another calibration point. It yielded U/Pb age spectra that suggest an igneous age of 89.5 ± 0.5 Ma (Fig. 9). By the TIMS-ID technique, it yielded externally concordant fractions with an age of 89.2 ± 0.1 Ma (Fig. 8). The igneous age for sample D9 is taken as 89.3 ± 0.2 Ma. Sample D10 yielded externally concordant ages suggesting an igneous age of 89.0 ± 0.5 Ma (Fig. 8). Sample D11 came from an area proximal to the proto–Kern Canyon fault (Fig. 2). It yielded an externally concordant age of 87.1 ± 0.4 Ma. The western edge of the D11 mass is progressively deformed and intruded by granitic dikes progressing westward into the proto–Kern Canyon fault.

The terminal phases of Domelands suite magmatism were dominated by the emplacement of widespread felsic dikes along with small tabular stocks of megacrystic granite bodies. This phase of Domelands suite magmatism is most pronounced north of latitude 35.75°N, and it is virtually absent in the southern reaches of the study area, as well as southward to the terminus of the Sierra Nevada batholith. Such magmatism is shown to have lasted locally to ca. 83 Ma and to have been focused along the northern segment of the proto–Kern Canyon fault (Busby-Spera and Saleeby, 1990).

Structural and age relations along the proto–Kern Canyon fault indicate that cessation of high-magnitude ductile strain was time transgressive during the emplacement of the Domelands suite. Detailed descriptions of the critical textural and structural relations are given elsewhere (Busby-Spera and Saleeby, 1990; Nadin, 2007; Nadin and Saleeby, this volume), but, here, we contribute data that are pertinent to the regional structural chronology. Sample D12 is from a mildly pegmatitic leucogranite dike from the southern segment of the proto–Kern Canyon fault damage zone. It crosscuts the mylonitic fabric at high-angle in the margin of the Claraville granodiorite, which is the local expression of the eastern domain of the proto–Kern Canyon fault. Sample D12 yielded two externally concordant fractions suggesting an igneous age of 86.1 ± 0.4 Ma (Fig. 8). These data in conjunction with the ages presented for the Claraville granodiorite constrain the main-phase ductile deformation along the southern segment of the proto–Kern Canyon fault to between ca. 86 and 92 Ma. Sample D13 is from a mylonitic pegmatitic granite dike that partially crosscuts and is partially transposed into the higher-strain blastomylonitic fabric of the Cannell Creek granite in the transition zone where Goldledge dikes progressively cut out the Cannell Creek granite northward (Fig. 2). This sample, therefore, records part of the ductile deformation history along this segment of the proto–Kern Canyon fault. Three natural size fractions as well as one abraded split of the intermediate size fraction yielded externally concordant ages suggesting an igneous age of 85.7 ± 0.5 Ma (Fig. 8). These data in conjunction with the age data presented already for the Cannell Creek granite bracket a significant component of the main-phase ductile deformation along the central segment of the proto–Kern Canyon fault to between ca. 85 and 94 Ma. As discussed further later, structural and age relations within the Goldledge granite indicate continued high-strain ductile deformation in intrusives of ca. 85 Ma age and a waning of ductile deformation at the time of the apparent ca. 83 Ma termination of Domelands magmatism.

The eastern zone of the Castle Rock unit, as well as the northeastern belt of the Claraville unit (Fig. 2), are cut by swarms of aplitic to pegmatitic leucogranite dikes as well as fine- to medium-grained equigranular granitic and granodioritic dikes. Sample D14 was taken from the largest equigranular granitic dike observed in the region. It yielded U/Pb age spectra that suggest an igneous age of 84.2 ± 1.5 Ma (Fig. 9). The three grains that yield ages of ca. 173 Ma resemble the principal inherited component observed in the nearby D6 Claraville sample. These, as well as the aberrant grain yielding an age of ca. 420 Ma, are interpreted here as source inheritance contaminants. The D14 age data, coupled with samples D12 and D13 and Goldledge granite data, suggest that felsic dike emplacement was widespread throughout the northern half of the Domelands suite between 86 and 83 Ma. Domelands suite magmatism was most prolific between 93 and 87 Ma, and it began locally as early as ca. 95 Ma. These age relations as well as structural and textural relations indicate that the Domelands suite was assembled over an ~10 m.y. time interval, and local dike emplacement continued for an additional ~2 m.y.

DISCUSSION

Integration of the geochronological data presented here with those of the Tehachapi complex (Saleeby et al., 1987, 2007; Pickett and Saleeby, 1994; Wood and Saleeby, 2008) provides a temporal framework that links the shallow batholithic and suprabatholithic volcanic levels of the study area to the lower-crustal complex. Such physical and temporal continuity along the oblique crustal section provides a basis to consider several important issues in Sierra Nevada batholith petrogenesis and tectonics, including: (1) composite batholith crustal structure; (2) magma production rates in Cordilleran-type arcs; (3) pluton emplacement mechanisms; (4) batholith compositional variations as fingerprints of source versus ascent and emplacement processes; and (5) kinematic relations of intra-arc deformation. Next, we discuss each of the problems from the perspective of the data that we have presented.

Crustal Structure and Magma Production Rates

Popular views on the crustal-scale structure of the Sierra Nevada batholith have embraced the idea that at mid-crustal levels (~10–20 km), the batholithic plutons spread out over a high-grade metamorphic country rock substrate (cf. Hamilton and Meyers, 1967). The physical continuity of the batholith down to ~35 km paleodepths of the Tehachapi complex and the seismic data across the shallow-level exposures of the Sierra Nevada batholith to the north of the study area, which resolve typical batholithic velocities down to current 35–40 km Moho depths (Ruppert et al., 1998; Fliedner et al., 2000), render this view obsolete. This study, the work referenced for the Tehachapi complex, and the seismic data indicate that ~90% of the Sierra Nevada batholith crust is consanguineous felsic batholith to at least 35 km. This takes into account ~10% outcrop area of pendant rocks observed at virtually all structural levels along the oblique crustal section. Petrogenetic data on lower-crust–upper-mantle xenoliths that were entrained in Neogene volcanic rocks erupted through shallow-level plutons of the central Sierra Nevada batholith indicate that the Cretaceous sub-batholithic seismic Moho was at ~45 km paleodepth, and that the petrologic Moho was at ~90 km depth (Ducea and Saleeby, 1998; Ducea, 2001; Saleeby et al., 2003). Xenoliths derived from the 35–90 km depth range are predominantly mafic-ultramafic residues and cumulates that are directly related to the overlying felsic batholith.

The large-scale crustal structure resolved for the southern Sierra Nevada batholith in conjunction with the age data provide constraints on arc magma production rates for this segment of the Cordilleran batholithic belt. The rates are best constrained for the Erskine Canyon sequence and Kern River/Bear Valley suite composite, which constitute a roughly coeval section of rocks extending from volcanic levels to ~35 km paleodepths. The along-strike dimension of this composite assemblage is ~100 km, and the across-strike width of the Bear Valley suite is ~50 km (Ross, 1989, 1995). If we take ~90% of this volume, considering exposures of pendant rocks and Early Cretaceous batholithic enclaves, we calculate a volume of ~157,500 km^3. Intrusion and eruption of this volume over the 105–98 Ma time interval yield a local felsic magma production rate of ~22,500 km^3/m.y., or ~0.023 km^3/yr. This magma production rate is ~0.25 of that observed over the past 25 yr for Kilauea volcano of the Hawaiian hot spot (Heliker and Mattox, 2003), and ~4 times the rate determined for oceanic-island arcs (Dimalanta et al., 2002).

The magma volume production rate determined for the Bear Valley–Kern River–Erskine Canyon volcano-plutonic crustal section corresponds to an intrusive flux rate of ~5×10^3 km^2/m.y. This is comparable to the 90 ± 5 Ma (peak) rate, and it is a factor of 10 greater than the 100 ± 5 Ma rate that was determined for ~1000 km length scales along the Cretaceous arc of California (Ducea, 2001). The 90 ± 5 Ma flux determined regionally is comparable to the local flux of the Domelands suite. The discrepancy between the local and regional 100 ± 5 Ma fluxes may arise from a regional bias in age determinations and map relations toward the younger 90 ± 5 Ma plutons of the better-exposed higher eastern Sierra, as well as the focused Laramide orogeny–related tectonic destruction of the older than 95 Ma arc rocks of the Southern California segment of the arc (cf. Saleeby, 2003).

Pluton Emplacement Mechanisms

Traditional views on the mechanisms of batholith emplacement embrace the concept of large middle- to upper-crustal magma chambers filling and ascending rapidly in largely molten states (Buddington, 1959; Pitcher and Berger, 1972; Paterson et al., 2008). Recent work in the central Sierra Nevada batholith has presented the alternative view that batholiths are emplaced incrementally, primarily by dike injections, and that large magma chambers are rare, or absent (Coleman et al., 2004; Glazner et al., 2004). Structural and age relations of the study area, coupled with those of the adjacent Tehachapi complex, suggest that a combination of both processes has operated in the southern Sierra Nevada batholith.

Evidence for incremental emplacement mechanisms is strong at both deep and shallow crustal levels. The tonalite of Bear Valley Springs is composed of a myriad of steeply dipping intrusive sheets and tabular wall-like plutons ranging from decimeter to kilometer scales. Neighboring intrusive bodies within the pluton are contrasted by subtle to pronounced textural and modal variations and both gradational and sharp contacts. Zircon age data indicate that this complex was assembled over the 102–98 Ma time interval. In contrast, at shallow crustal levels in the Bear Valley Suite, the Mount Adelaide and Poso Flat units only locally show internal contacts, and their contacts with the Bear Valley Springs unit typically cut across the Bear Valley Springs primary structure. In the Domelands suite, at <5 kbar levels, the Castle Rock granites consists of a myriad of steeply dipping dikes and small tabular plutons. Age, structural, and textural relations show that even the megacrystic granites were emplaced as a series of intrusions. The megacrystic granites and finer-grained felsic dikes were emplaced over the time interval of 83–89 Ma. Likewise, the oldest phases of the Domelands suite, granites of Long Meadow, Cannell Creek, and Onyx, were emplaced as a series of small tabular plutons and dikes. In contrast, the deeper-level, 90–93 Ma Claraville granodiorite exhibits mainly larger-scale primary structure, suggesting the coalescence of relatively large magma batches with only minor petrologic variations. At map scale, these are comparable in size to the plutons that constitute the Needles intrusive suit as well as the Mount Adelaide and Poso Flat units of the Bear Valley suite (Fig. 2). These typically underlie map areas of roughly 50 km^2. Additional detailed work could reveal, however, that these larger bodies are also composed of multiple internal units.

Exposure quality of much of the study area inhibits detailed resolution of the three-dimensional structure of many of the plutons. The Bear Valley Springs tonalite and the Castle Rock granites are dominated by steeply dipping internal intrusive contacts. In the case of the Castle Rock complex, this structure is controlled

by the proto–Kern Canyon fault in the west, and shallow-crustal-level tensile fractures throughout, which controlled felsic dike emplacement. Primary structure within the deeper-level Claraville unit suggests that its internal bodies are steeply oriented. The older phases of the South Fork suite possess internal and wallrock structural relations that suggest they were emplaced as relatively small diapirs (Saleeby and Busby-Spera, 1986, 1993; Zeng et al., 2005). Age data presented herein and structural relations further indicate that the most aerially extensive Rabbit Island pluton of the suite continued to grow incrementally over the 98–94 Ma time interval after its principal diapiric phase by dike and possible smaller-scale diapir emplacement. Resolution of the primary shape of the Mount Adelaide and Poso Flat units, and the various plutons of the Needles and Kern River suites, is important for understanding primary batholithic structure as well as for determining slip on the Kern Canyon fault and proto–Kern Canyon fault. As noted previously, the shallowest structural levels of the Bear Valley Springs unit appear as a series of commingled tonalitic and gabbroic sill-like bodies dipping under a roof of Kern River suite intrusives and pendant rock. These Bear Valley Springs outliers were split off from the deeper levels of the Bear Valley Springs unit by the Poso Flat unit and plutons of the Needles suite (Fig. 2). This presents the possibility that these shallower-level plutons, relative to the main Bear Valley Springs complex, are a series of horizontally, and or low-dipping, stacked sill-like bodies lying above Bear Valley Springs–like vertical structure. If such were the case, the magma volumes represented by each of the shallower-level plutons could be relatively small in relation to their map-view areas. Images of vertically sheeted deep-level batholithic structure transitioning at upper-crustal levels to horizontally stacked sill-like bodies are presented in Brown and McClelland (2000), Sisson et al. (1996), and Saleeby et al. (2003). Mid- to deep-crustal seismic anisotropy resolved across shallow levels of the central to southern Sierra Nevada batholith (Ruppert et al., 1998) is consistent with strong vertical preferred orientations in batholithic structure at depth, which, based on the corresponding surface structure, lies beneath plutons that, in map view, are ellipsoidal shallow-level structures.

The rapid ascent of relatively large batches of magma (>10 km^3) to shallow levels during the construction of the Sierra Nevada batholith is recorded in metavolcanic remnants of the southern Sierra Nevada batholith, like those of the Erskine Canyon sequence. The effusive members of such remnants are dominated by voluminous silicic ignimbrites and subordinate andesitic associations (Fiske and Tobisch, 1978, 1994; Busby-Spera, 1984; Tobisch et al., 1986, 2000; Hanson et al., 1987; Saleeby et al., 1990). These relations suggest that large-volume ignimbrite eruptions from calderas dominated over incremental construction of andesitic stratacones. Plutons and metavolcanic rocks of the study area, and apparently much of the greater Sierra Nevada batholith, thus record basement construction at virtually all crustal levels by the emplacement of large numbers of small magma batches, and progressively smaller numbers of larger batches. Some of these batches were quite large and may have resembled traditional views of relatively large magma chambers. The predominance of large-volume ignimbrites over andesitic stratacones as the dominant effusions of the Sierra Nevada batholith arc further argues for the ascent of larger magma batches to the upper crust. This observation, in conjunction with the predominance of small- to intermediate-size plutonic masses over large-size masses, suggests that there may be an upper size limit on magma bodies that can make it to the upper crust without promoting their own eruption.

Magma Source, Ascent, and Solidification Regimes, and Compositional Variations

A corollary to the large-volume mid- to upper-crustal magma chamber model for batholith formation is the potential for the development of significant intrapluton compositional variations by some combination of fractionation and wallrock assimilation (cf. Bateman and Chappell, 1979; Kistler et al., 1986; Frost and Mahood, 1987). Field relations in and zircon age data from the study area put severe limitations on the extent to which the corresponding magmatic systems were modified by wallrock assimilation at solidification level. Wallrock xenoliths are rare in the region, both at shallow and deep crustal levels. Mafic inclusions, or xenoliths, are most readily explained as having been derived from the commingling of mafic dikes, and where U/Pb zircon ages have been determined on such inclusions, they are the same as those of the host granitoids (Chen and Moore, 1982). In zones of wallrock migmatization by plutons of the South Fork suite, zircon assimilation and modification of pluton Nd and Sr isotopic systematics are not observed to extend >100 m into the respective plutons (Zeng, 2003; Zeng et al., 2005). At deep crustal levels, within the Bear Valley suite and Early Cretaceous orthogneisses of the Tehachapi complex, zircon assimilation and Nd-Sr isotopic modifications are observed to extend at <100 m scales into both granitoids and gabbroids, adjacent to 100-m- to 1-km-scale migmatitic pendants (Saleeby et al., 1987; Pickett and Saleeby, 1994). The relationships outlined already indicate that wallrock assimilation over a wide range of exposure depths is not a first-order process in producing map-scale compositional variations of the plutons. The limited assimilation patterns observed along the oblique crustal section also suggest that source inheritance dominates over ascent entrainment as the dominant zircon discordance mechanism in the study area.

The delivery of metasedimentary wallrock materials into the magmatic source regime of the Sierra Nevada batholith is well recorded in the radiogenic and stable isotopes of the batholiths mafic granulite–garnet pyroxenite residue assemblage, sampled as xenoliths by Neogene volcanics (Ducea and Saleeby, 1998; Ducea, 2001). The majority of such xenoliths show that such supracrustal components have been homogenized with mantle and lower-crustal igneous/meta-igneous components. Such homogenization is further recorded in elevated $\delta^{18}O$ values of zircon from both deep- and shallow-level Sierra Nevada batholith granitoids and gabbroids (Lackey et al., 2005). Nevertheless, sig-

nificant variations in radiogenic isotopes within large plutons like the tonalite of Bear Valley Springs (Saleeby et al., 1987; Kistler and Ross, 1990; Pickett and Saleeby, 1994), and the Tuolumne intrusive suite of the central Sierra Nevada batholith (Kistler et al., 1986) indicate that for at least some large magma batches, source homogenization may be incomplete, and/or the source components may change over relatively short time scales relative to the incremental growth cycles of the plutons.

The high degree of source homogenization suggested by the xenolith data coupled with the lack of evidence for significant assimilation at shallow-levels, along with other lines of evidence, suggest that the deep levels of the ascent regime may be a fertile environment for limited assimilation and compositional modification of magmas. This is suggested by coupled U/Pb zircon systematics and Sr_i data from the deep-level Bear Valley suite rocks as contrasted to those of the shallower-level Bear Valley suite rocks as well as those of the Needles suite (Fig. 10). Field observations and U/Pb age data from the deep-level rocks reveal zones of assimilation of partial melt products into Bear Valley suite intrusives both from Early Cretaceous orthogneisses and metasedimentary pendants (Saleeby et al., 1987, 2007). The tonalite of Bear Valley Springs over its entire 2–8 kbar exposure levels shows an order-of-magnitude greater Sr_i variation than the entire Needles suite (Saleeby et al., 1987; Kistler and Ross, 1990; Pickett and Saleeby, 1994). Within this range, the relatively shallow-level Mount Adelaide and Poso Flat members of the Bear Valley suite, like plutons of the Needles suite, show a much tighter clustering of Sr_i values than the deeper-level Bear Valley Springs unit (Fig. 10). This raises the possibility that assimilation and compositional modification of magmas under some circumstances occurs in the lower crust following ascent from the source regime.

Observations along the oblique crustal section suggest that vertical primary structures pervade the Sierra Nevada batholith at lower crustal levels. These consist of steeply dipping tabular wall-like masses of tonalite with stretched mafic inclusion swarms and partially disrupted comagmatic mafic dikes, and bounding vertical screens of thinly sheeted mafic and felsic intrusives as well as

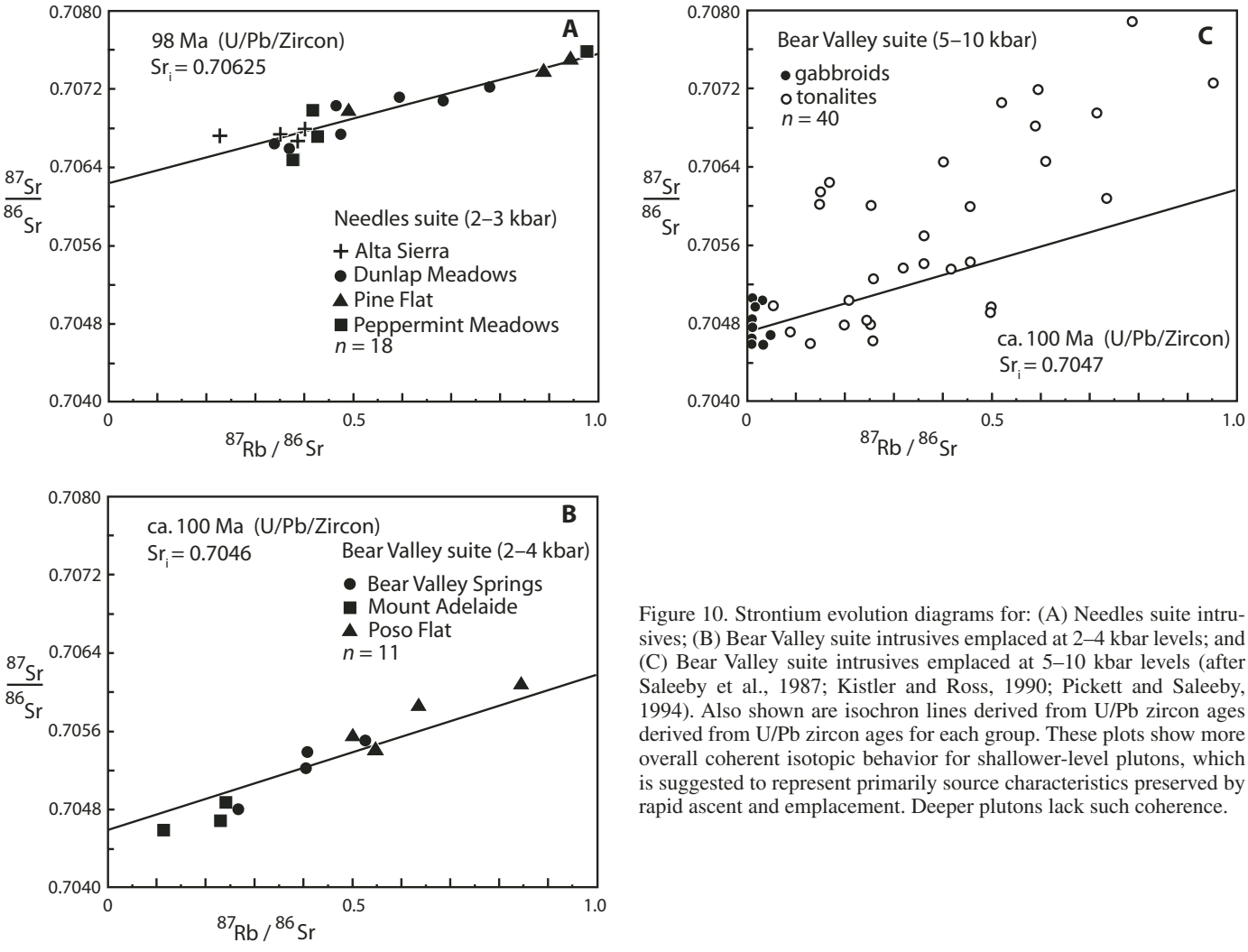

Figure 10. Strontium evolution diagrams for: (A) Needles suite intrusives; (B) Bear Valley suite intrusives emplaced at 2–4 kbar levels; and (C) Bear Valley suite intrusives emplaced at 5–10 kbar levels (after Saleeby et al., 1987; Kistler and Ross, 1990; Pickett and Saleeby, 1994). Also shown are isochron lines derived from U/Pb zircon ages derived from U/Pb zircon ages for each group. These plots show more overall coherent isotopic behavior for shallower-level plutons, which is suggested to represent primarily source characteristics preserved by rapid ascent and emplacement. Deeper plutons lack such coherence.

high-grade pendants. An analogous vertical structure is resolved at deep crustal levels beneath shallow-level plutons of the central Sierra Nevada batholith by seismic anisotropy (Ruppert et al., 1998). Crustal-scale thermal models of the Sierra Nevada batholith indicate that at >20 km depths, solidified plutons remain at near-solidus conditions for million-year time scales (Barton and Hanson, 1989), and thus the deep batholithic rocks themselves under such conditions constitute a labile environment for successive magma pulses to interact with. Large excursions in Sr_i and i/e patterns of zircon in a subordinate number of intrusive bodies of the Bear Valley Springs tonalite are suggested to have arisen from the proximal assimilation of partial melts from migmatitic metasedimentary septa as well as older (Early Cretaceous) deep-batholithic granitoids. Such compositionally modified zones of the tonalite are suggested to be largely the remnants of relatively small magma batches that stagnated at deep crustal levels and that partially assimilated local host melt products. Shallow levels of the Bear Valley Springs unit as well as the Mount Adelaide and Poso Flat units, and the entire Needles suite, in this view, represent little-modified, larger-volume magma batches. As shown on Figure 10, these shallower-level units yield reasonably coherent isochron patterns on Sr evolution diagrams with apparent age significance, whereas the deeper-level rocks are do not. This suggests that the shallower, and possibly more rapidly ascended, plutons better preserve source characteristics than the myriad of smaller deeper-level intrusions.

Discordance patterns in U/Pb zircon ages reported here are considered to be primarily the result of source inheritance. Implicit in the systematic discussions given here for the zircon samples is the fact that few, if any, of the samples exhibiting discordances can be spatially related to proximal metamorphic pendants that could have conceivably rendered a zircon assimilation component. Caveats are issued here for the highly contaminated zones of South Fork suite plutons, and the local-scale assimilations noted for the deep-level rocks discussed already. Discordances arising from the incorporation of detrital zircon from metaclastic sources are readily resolved by steep discordance trajectories projecting toward the dominant Proterozoic detrital component (cf. samples E3, E5, E6, K7, and D5). For the ICP-MS data, such discordances are recorded in the highly aberrant data points that yield Proterozoic and Paleozoic(?) U/Pb ages (samples D6 and D14 [Fig. 9], and E7, K3, N1, N9, and D7 [Table DR3—see footnote 1]).

Discordances arising from the incorporation of batholithic zircon from earlier cycles have important petrogenetic implications as well. Of particular interest are samples D6 and D14, which yielded secondary U/Pb age clusters in the Jurassic. These samples are located along the eastern margin of the Domelands suite, adjacent to a dense cluster of Jurassic and Triassic plutons that constitute the southeastern edge of the Sierra Nevada batholith (Fig. 1). No other early Mesozoic plutons have been found to the west of this cluster, even as far south and west as the Tehachapi complex. This suggests that the source regime for the Domelands suite in part overlapped with the deep levels of the early Mesozoic Sierran arc. Such recycling of earlier-cycle deep-level arc rocks appears to be more important in the study area and the Tehachapi complex for the locus of the Early Cretaceous Sierra Nevada batholith. Discordance effects arising from the incorporation of zircon derived from earlier Cretaceous plutonic rocks are difficult to resolve in the ID-TIMS data, but they are clearly resolved in the ICP-MS data. Samples N9 and D6 yielded secondary U/Pb age clusters of Early Cretaceous age, and many samples (K5, B3, B6, B7, N1, N7, N8, S7, D3, and D7) yielded slightly discordant U/Pb ages that are displaced above the mid- to Late Cretaceous igneous age means. Such inheritance patterns suggest that previously crystallized arc plutons, and/or fairly evolved cumulate masses left from ascended arc plutons, comprise a nontrivial source component for the large-volume Middle to Late Cretaceous Sierra Nevada batholith.

Chronology of Regional Deformation

U/Pb zircon age data presented here in conjunction with other geochronological and structural studies help to constrain the timing and kinematic relations of regional deformation that affected the southern Sierra Nevada batholith. In terms of relative chronology, the principal structures of the study area include: (1) prebatholithic ductile deformation, including folding, thrusting, and cleavage development of the Kings sequence pendant rocks; (2) at least local brittle high-angle faulting and uplift of the Kings sequence, and unconformable overlap by the Erskine Canyon sequence; (3) high-magnitude ductile strain and local migmatization of pendant rocks in conjunction with the intrusion of the South Fork intrusive suite; (4) east-side-up ductile thrusting along the proto–Kern Canyon fault; (5) dextral-sense ductile shear and displacement along the proto–Kern Canyon fault as well as the Kern Canyon fault; and (6) brittle deformation along the Kern Canyon and related faults. The age data that we have presented here place relatively tight absolute constraints on items two through five, and only bounding constraints on one and six. Next, we focus on items two, four, and five.

The evolution of the proto–Kern Canyon fault is an essential factor in the tectonics of the southern Sierra Nevada batholith. The proto–Kern Canyon fault is distinguished from the Kern Canyon fault by a wide zone of ductile deformation (1–4 km) versus more focused brittle and local ductile deformation of the Kern Canyon fault, and by a southward bifurcation of the two structures at latitude ~35.75°N (Fig. 2). Dextral slip on the Kern Canyon fault in the study area is resolved at 12 ± 1 km, and dextral displacement resulting from ductile shear strain along the proto–Kern Canyon fault is estimated at ~15 km (Nadin and Saleeby, this volume). This leads to a net dextral displacement of ~27 km along the system north of ~35.75°N, and ~15 km along the southern proto–Kern Canyon fault. Age data presented here and in Busby-Spera and Saleeby (1990) and structural and thermochronological data reviewed in Nadin and Saleeby (this volume) put some useful absolute constraints on this displacement history. The 94.7 ± 0.4 Ma Cannell Creek granite (sample D2) records high-

temperature early-stage downdip shear. Local and regional structural relations indicate that this downdip shear occurred in association with a pronounced phase of early-stage west-directed ductile thrusting along the shear zone, and that such deformation abruptly evolved into dextral shear. Our structural and textural studies of the Cannell Creek granite as well as $^{40}Ar/^{39}Ar$ hornblende and biotite thermochronologic studies (Dixon, 1995; Wong, 2005) indicate that this kinematic change occurred while the Cannell Creek granite was cooling through hot subsolidus conditions. The transition occurred at ca. 90 Ma. The Goldledge granite cuts out the northern end of the Cannell Creek granite where the latter is pervasively sheared in a dextral sense. Dikes and concordant intrusive sheets of the Goldledge granite record progressively less dextral shear through time than that of the Cannell Creek pluton by the 85.7 ± 0.5 Ma age of sample D13 mylonite, descending in age and intensity of strain to the 85 ± 1 Ma mylonitic and 83 ± 1 Ma protomylonitic Goldledge rocks studied by Busby-Spera and Saleeby (1990). In contrast, the sample D12 leucogranite dike, which is nondeformed and cuts the proto–Kern Canyon fault fabric along the west margin of the Claraville pluton to the south, appears to limit such ductile deformation along the southern proto–Kern Canyon fault to between 92.5 ± 0.7 (sample D4 taken as host age) and the 86.1 ± 0.4 Ma age of the D12 dike (Fig. 2; Table 1). It is suggested that the southern segment of the proto–Kern Canyon fault became inactive at the time that Kern Canyon fault dextral displacements were initiated and were shunted into the northern segment of the shear zone, and that this was coincident with the initiation of Goldledge granite emplacement (Nadin and Saleeby, this volume).

The total offset history of the proto–Kern Canyon fault is obscure due to the fact that a significant component of its history may predate the emplacement of its east-bounding 90–85 Ma large-volume plutons, particularly to the north. Vertical components of slip, which have affected these as well as older plutons, have imparted significant along-strike variations in the depth of exposure gradients of the oblique crustal section along opposing walls of the proto–Kern Canyon fault (Ague and Brimhall, 1988; Nadin and Saleeby, this volume). This pattern and the fact that the regional trace of the $Sr_i = 0.706$ isopleth of the Sierra Nevada batholith coincides with the southern ~50 km of the proto–Kern Canyon fault (Fig. 1) (Kistler and Ross, 1990; Pickett and Saleeby, 1994) suggests that it is a much more fundamental structure than that implied by the dextral displacements noted previously.

Evidence of a possible earlier largely cryptic displacement phase along the proto–Kern Canyon fault was discussed by Busby-Spera and Saleeby (1990). It was noted that the ignimbrites of the 105–102 Ma Erskine Canyon sequence were ponded against a steep buttress unconformity along with fans of local basement-derived talus breccias (Fig. 3), and that such ponding occurred under subaqueous conditions. Inasmuch as the remnants of the Late Cretaceous shoreline lie in the Great Valley subsurface to the west (Ingersoll, 1979, 1982), such subaqueous conditions are likely to record a lacustrine environment. Furthermore, the homoclinal volcanic section dips into, and becomes pervasively sheared eastward into, the principal ductile damage zone of the proto–Kern Canyon fault. This prompted the suggestion that the Erskine Canyon sequence accumulated in a dextral-slip fault-controlled volcano-tectonic depression along a trench-linked transform, akin to those that form in arcs above zones of oblique subduction (Fitch, 1972; Jarrard, 1986). If such speculation is correct, then this "window" into the early kinematic history of the proto–Kern Canyon fault may also represent a remnant of the heretofore cryptic Mojave–Snow Lake fault, a hypothetical large magnitude intra-arc dextral-slip fault of Early Cretaceous age that is postulated to have been responsible for the offset of metamorphic pendant rocks along the axial Sierra Nevada batholith (Lahren and Schweickert, 1989).

The temporal relations of ductile thrusting and dextral shear along the proto–Kern Canyon fault may be correlated to the timing and kinematic patterns of regional deformation of the Tehachapi complex to the south of the study area, and the central Sierra Nevada batholith to the north. In the Tehachapi complex, crustal thickening related to the onset of intra-arc thrusting commenced between 90 and 100 Ma, and vigorous uplift and unroofing of the deep-level batholithic rocks were operative between 90 and 94 Ma (Saleeby et al., 2007). This study, in conjunction with that of Grove et al. (2003), also shows that the subduction-accretion assemblages of the Rand schist were displaced eastward by regional low-angle subduction from the Franciscan trench to beneath the Tehachapi complex between 86 and 93 Ma. The timing of such lithosphere-scale thrusting and compressional deformation matches well with ca. 95 Ma onset of ductile thrusting along the proto–Kern Canyon fault and its ca. 86 Ma termination along its southern segment. In the central Sierra Nevada batholith, steeply dipping west-directed reverse-sense ductile shear zones were active between 90 and 100 Ma, and dextral-sense ductile shear zones were active primarily between 80 and 90 Ma (Tobisch et al., 1995). These also match the thrust-dominated and dextral-dominated deformation phases of the proto–Kern Canyon fault, although ductile shear along the proto–Kern Canyon fault was waning by ca. 83 Ma. Brittle overprints of the Kern Canyon fault superimposed across the northern segment of the proto–Kern Canyon fault could correspond to continuing ductile deformation to the north as young as ca. 78 Ma. Rapid unroofing of the southernmost Sierra Nevada batholith in the 85–95 Ma time interval may account for embrittlement of the post–83 Ma dextral shear, while slower unroofing to the north may account for a more protracted interval of ductile deformation.

Finally, the intense history of intra-arc deformation and unroofing that is recorded for the southern Sierra Nevada batholith is also recorded in the depositional history of the Great Valley forearc basin, as well as in some metaclastic rocks of the Franciscan complex. Petrographic and stratigraphic studies of the Great Valley forearc sequence reveal an acceleration of Sierra Nevada batholith unroofing that commenced in strata that are roughly constrained to be 90 Ma in age (Mansfield, 1979). Furthermore, the entire late Mesozoic forearc basin sequence was eroded off the southernmost Great Valley between Late Cretaceous and Paleo-

cene time (Reid and Cox, 1989), presumably in parallel with crustal-scale tilting and exhumation of the southernmost Sierra Nevada batholith oblique crustal section. Rapid unroofing of the southern Sierra Nevada batholith and the adjacent Southern California batholith is also recorded by U/Pb ages of detrital zircon from Upper Cretaceous strata of the southern Franciscan complex and the Rand and related schists that tectonically underlie the Tehachapi complex and Southern California batholith (Barth et al., 2003; Grove et al., 2003; Jacobson et al., 2004). Thus, a regionally coherent story is emerging concerning the timing and kinematics of Late Cretaceous intra-arc deformation and related unroofing of the central to southernmost Sierra Nevada batholith.

SUMMARY AND CONCLUSIONS

We present an extensive U/Pb zircon age data set for the southern Sierra Nevada batholith and partly coeval/cogenetic silicic metavolcanic rocks preserved as an unconformable "keel" that was deposited on pre-Cretaceous metamorphic framework rocks. These data tie together earlier published, regionally extensive U/Pb zircon age data sets from the central Sierra Nevada batholith to the north and the deep-level batholithic rocks of the Tehachapi complex to the south. These data, in conjunction with regional field mapping, establish physical continuity and temporal continuity in pluton emplacement along an oblique crustal section traversing volcanic and shallow-level plutonic levels in the north to lower-crustal batholithic (~35 km) levels in the south. The establishment of such continuity, along with the details of the age relations, provides a framework for further analysis of a series of issues in batholith primary structure, pluton emplacement mechanisms, factors influencing the compositional evolution of batholithic magmas, and regional deformations superimposed on the southern Sierra Nevada batholith.

Based on the U/Pb zircon age data, our own mapping, and the mapping and derivative petrographic/geochemical data of published studies (Saleeby et al., 1987, 2007; Ross, 1989, 1995; Kistler and Ross, 1990), we define five intrusive suites in the southern Sierra Nevada batholith between latitudes 35°N and 36.2°N. These consist of: (1) the granitic Kern River suite (102–105 Ma); (2) the tonalitic to gabbroic Bear Valley suite (ca. 102–98 Ma); (3) the gabbroic to granodioritic South Fork suite (ca. 94–100 Ma); (4) the tonalitic to granodioritic Needles suite (101–95 Ma); and (5) the granitic Domelands suite (83–95 Ma). The Kern River suite is the subvolcanic intrusive complex for the 102–105 Ma Erskine Canyon silicic volcanic-hypabyssal sequence. The Kern River suite is intruded by both the Bear Valley and Needles suites. These three suites are restricted to the west side of the proto–Kern Canyon fault, a complex ductile shear zone that records both dextral strike-slip and west-directed thrust deformation along the axial zones of the southern Sierra Nevada batholith. The South Fork and Domelands intrusive suites lie to the east of the proto–Kern Canyon fault, and the Domelands suite was emplaced incrementally during the principal ductile deformation history of the proto–Kern Canyon fault.

Age and structural relations indicate that east-side-up ductile thrusting along the proto–Kern Canyon fault commenced possibly as early as ca. 95 Ma, and that dextral shear commenced by ca. 90 Ma. The southern segment of the shear zone and the northern segment are differentiated by the merging of the Kern Canyon fault into the proto–Kern Canyon fault at latitude ~35.75°N. Dextral ductile shear was waning along the northern segment of the shear zone by ca. 83 Ma, and it was terminated by ca. 86 for the southern segment. The prolonged history of dextral shear along the northern segment relative to the southern segment corresponds with the shunting of the Kern Canyon fault into the northern segment of the system as the southern segment of the proto–Kern Canyon fault became inactive. Dip-slip components of displacement along the proto–Kern Canyon fault have resulted in two different paleodepth gradients within its opposing walls along the southern Sierra Nevada batholith oblique crustal section.

Regional patterns in pluton emplacement and deformation along the proto–Kern Canyon fault may be correlated in time to analogous pluton emplacement patterns and deformations of the central Sierra Nevada batholith. These may be further correlated with deformation and unroofing of the deepest exposed levels of the Sierra Nevada batholith to the south and the low-angle underthrusting and tectonic underplating of Franciscan subduction-accretion assemblages beneath the deep-level rocks. This deformation history is also recorded in the depositional history of the adjacent Great Valley forearc basin, and in some metaclastic units of the southern Franciscan subduction complex.

ACKNOWLEDGMENTS

This research was funded by National Science Foundation (NSF) grants EAR-98-15024 and EAR-02-30383 and a grant from the Gordon and Betty Moore Foundation awarded to Saleeby, and EAR-00-87125 and EAR-02-29470 awarded to Ducea. The parallel research efforts of D.C. Ross and R.W. Kistler greatly enhanced this research. Field assistance from Kyle Bradley, Sara Cina, Cary Gazis, and Gweltaz Maheo, and drafting and field assistance by Zorka Saleeby are kindly acknowledged. Reviews of an early draft of this manuscript by Bill McClelland and Elizabeth Miller were helpful. Special thanks are due to C.A. Hopson, who greatly stimulated the senior author to pursue basement geochronology applied to problems in tectonics and petrogenesis. This is Caltech Tectonics Observatory contribution 50.

REFERENCES CITED

Ague, J.J., 1997, Thermodynamic calculation of emplacement pressures for batholithic rocks, California: Implication for the aluminum-in-hornblende barometer: Geology, v. 25, p. 563–566, doi: 10.1130/0091-7613(1997)025<0563:TCOEPF>2.3.CO;2.

Ague, J.J., and Brimhall, G.H., 1988, Magmatic arc asymmetry and distribution of anomalous plutonic belts in the batholiths of California: Effects of assimilation, crustal thickness, and depth of crystallization: Geological Society of America Bulletin, v. 100, p. 912–927, doi: 10.1130/0016-7606(1988)100<0912:MAAADO>2.3.CO;2.

Barth, A.P., and May, D.J., 1992, Mineralogy and pressure-temperature-time path of Cretaceous granulite gneisses, southeastern San Gabriel Mountains, Southern California: Journal of Metamorphic Geology, v. 10, p. 529–544.

Barth, A.P., Wooden, J.L., Grove, M., Jacobson, C.E., and Pedrick, J.N., 2003, U-Pb zircon geochronology of rocks in the Salina Valley region of California: A reevaluation of the crustal structure and origin of the Salinian block: Geology, v. 31, p. 517–520, doi: 10.1130/0091-7613(2003)031<0517:UZGORI>2.0.CO;2.

Barton, M.D., and Hanson, R.B., 1989, Magmatism and the development of low-pressure metamorphic belts: Implications from the western United States and thermal modeling: Geological Society of America Bulletin, v. 101, p. 1051–1065, doi: 10.1130/0016-7606(1989)101<1051:MATDOL>2.3.CO;2.

Bateman, P.C., 1983, A summary of critical relations in the central part of the Sierra Nevada batholith, California, USA, *in* Roddick, J.A., ed., Circum-Pacific Plutonic Terranes: Geological Society of America Memoir 159, p. 241–254.

Bateman, P.C., and Chappell, B.P., 1979, Crystallization, fractionation, and solidification of the Tuolumne intrusive series, Yosemite National Park, California: Geological Society of America Bulletin, v. 90, p. 465–482, doi: 10.1130/0016-7606(1979)90<465:CFASOT>2.0.CO;2.

Bateman, P.C., and Clark, L.D., 1974, Stratigraphic and structural setting of Sierra Nevada batholith: Pacific Geology, v. 8, p. 79–89.

Behr, W., and Dunne, G.C., 2006, Evidence for multiple strands of the late Paleozoic truncational fault of North America within exposures of the Kennedy Meadows pendant: Sierra Nevada, California: Geological Society of America Abstracts with Programs, v. 38, no. 5, p. 11.

Brown, E.H., and McClelland, W.C., 2000, Pluton emplacement by sheeting and vertical ballooning in part of the southeast Coast plutonic complex, British Columbia: Geological Society of America Bulletin, v. 112, p. 708–719, doi: 10.1130/0016-7606(2000)112<0708:PEBSAV>2.3.CO;2.

Buddington, A.F., 1959, Granite emplacement with special reference to North America: Geological Society of America Bulletin, v. 70, p. 671–747.

Busby-Spera, C.J., 1984, Large-volume rhyolite ash flow eruptions and submarine caldera collapse in lower Mesozoic Sierra Nevada, California: Journal of Geophysical Research, v. 89, p. 8417–8427.

Busby-Spera, C., and Saleeby, J.B., 1990, Intra-arc strike-slip fault exposed at batholithic levels in southern Sierra Nevada, California: Geology, v. 18, p. 255–259.

Chen, J.H., and Moore, J.G., 1982, Uranium-lead isotopic ages from the Sierra Nevada batholith: Journal of Geophysical Research, v. 87, p. 4761–4784.

Clemens-Knott, D., and Saleeby, J.B., 1999, Impinging ring dike complexes in the Sierra Nevada batholith, California: Roots of the Early Cretaceous volcanic arc: Geological Society of America Bulletin, v. 111, no. 4, p. 484–496, doi: 10.1130/0016-7606(1999)111<0484:IRDCIT>2.3.CO;2.

Coleman, D.S., and Glazner, A.F., 1998, The Sierra crest magmatic event: Rapid formation of juvenile crust during the Late Cretaceous in California, *in* Ernst, W.G., and Nelson, C.A., eds., Integrated Earth and Environment Evolution of the Southwestern United States: Columbia, Maryland, Bellwether Publishing Ltd., p. 253–272.

Coleman, D.S., Gray, W., and Glazner, A.F., 2004, Rethinking the emplacement and evolution of zoned plutons: Geochronologic evidence for incremental assembly of the Tuolumne intrusive suite, California: Geology, v. 32, p. 433–436, doi: 10.1130/G20220.1.

Dickinson, W., and Gehrels, G.E., 2003, U-Pb ages of detrital zircons from Permian and Jurassic eolian sandstones of the Colorado Plateau, USA: Paleogeographic implications: Sedimentary Geology, v. 163, p. 29–66, doi: 10.1016/S0037-0738(03)00158-1.

Dickinson, W., and Snyder, W.S., 1978, Plate tectonics of the Laramide orogeny, *in* Mathews, V., III, ed., Laramide folding associated with basement block faulting in the western United States: Geological Society of America Memoir 151, p. 335–366.

Dimalanta, C., Taira, A., Yumul, G.P., Jr., Tokuyama, H., and Mochizuki, K., 2002, New rates of western Pacific island arc magmatism from seismic and gravity data: Earth and Planetary Science Letters, v. 202, p. 105–115, doi: 10.1016/S0012-821X(02)00761-6.

Dixon, E.T., 1995, $^{40}Ar/^{39}Ar$ Hornblende Geochronology and Evaluation of Garnet and Hornblende Barometry, Lake Isabella, the Tehachapi Area, Southern Sierra Nevada, California [M.S. thesis]: Ann Arbor, University of Michigan, 63 p.

du Bray, M.N., and Dellinger, D.A., 1981, Geologic Map of the Golden Trout Wilderness, Southern Sierra Nevada, California: U.S. Geological Survey Miscellaneous Field Studies Map MF-1231-a, scale 1:48,000.

Ducea, M., 2001, The California arc: Thick granitic batholiths, eclogitic residues, lithospheric-scale thrusting, and magmatic flare-ups: GSA Today, v. 11, no. 11, p. 4–10, doi: 10.1130/1052-5173(2001)011<0004:TCATGB>2.0.CO;2.

Ducea, M.N., and Saleeby, J.B., 1996, Buoyancy sources for a large, unrooted mountain range, the Sierra Nevada, California; evidence from xenolith thermobarometry: Journal of Geophysical Research, v. 101, p. 8229–8244, doi: 10.1029/95JB03452.

Ducea, M.N., and Saleeby, J.B., 1998, The age and origin of a thick mafic-ultramafic keel from beneath the Sierra Nevada batholith: Contributions to Mineralogy and Petrology, v. 133, p. 169–185, doi: 10.1007/s004100050445.

Dunne, G.C., and Saleeby, J.B., 1993, Kern Plateau shear zone, southern Sierra Nevada—New data concerning age and northward continuation: Geological Society of America Abstracts with Programs, v. 25, no. 5, p. 33.

Evernden, J.F., and Kistler, R.W., 1970, Chronology of Emplacement of Mesozoic Batholithic Complexes in California and Western Nevada: U.S. Geological Survey Professional Paper 623, 42 p.

Fiske, R.S., and Tobisch, O.T., 1978, Paleogeographic significance of volcanic rocks of the Ritter Range pendant, central Sierra Nevada, California, *in* Howell, D.G., and McDougal, K.A., eds., Mesozoic Paleogeography of the Western United States: Sacramento, California, Society of Economic Paleontologists and Mineralogists, Pacific Section, Pacific Coast Paleogeography Symposium 2, p. 209–219.

Fiske, R.S., and Tobisch, O.T., 1994, Middle Cretaceous ash-flow tuff and caldera collapse deposit in the Minarets Caldera, east-central Sierra Nevada, California: Geological Society of America Bulletin, v. 106, p. 582–593, doi: 10.1130/0016-7606(1994)106<0582:MCAFTA>2.3.CO;2.

Fitch, T.J., 1972, Plate convergence, transcurrent faults, and internal deformation adjacent to Southeast Asia and the western Pacific: Journal of Geophysical Research, v. 77, p. 4432–4460.

Fliedner, M.M., Klemperer, S.L., and Christensen, N.I., 2000, Three-dimensional seismic model of the Sierra Nevada arc, California, and its implications for crustal and upper mantle composition: Journal of Geophysical Research, v. 105, p. 10,899–10,921, doi: 10.1029/2000JB900029.

Frost, T.P., and Mahood, C.A., 1987, Field, chemical, and physical constraints on mafic-felsic magma interaction in the Lamark granodiorite, Sierra Nevada, California: Geological Society of America Bulletin, v. 99, p. 272–291, doi: 10.1130/0016-7606(1987)99<272:FCAPCO>2.0.CO;2.

Glazner, A.F., Bartley, J.M., Coleman, D.S., Gray, W., and Taylor, R.Z., 2004, Are plutons assembled over millions of years by amalgamation from small magma chambers: GSA Today, v. 14, no. 5, p. 4–11.

Grove, M., Jacobson, C.E., Barth, A.P., and Vucic, A., 2003, Temporal and spatial trends of Late Cretaceous–early Tertiary underplating of Pelona and related schist beneath Southern California and southwestern Arizona, *in* Johnson, S.E., Paterson, S.R., Fletcher, J.M., Girty, G.H., Kimbrough, D.L., and Martin, B.A., eds., Tectonic Evolution of Northwestern Mexico and the Southwestern USA: Geological Society of America Special Paper 374, p. 381–406.

Hamilton, W., and Meyers, W.B., 1967, The Nature of Batholiths: U.S. Geological Survey Professional Paper 554-C, 30 p.

Hanson, R.B., Saleeby, J.B., and Fates, D.G., 1987, Age and tectonic setting of Mesozoic metavolcanic and metasedimentary rocks, northern White Mountains, California, and origin of the Barcroft structural break: Geology, v. 15, p. 1074–1078, doi: 10.1130/0091-7613(1987)15<1074:AATSOM>2.0.CO;2.

Heliker, C., and Mattox, T.N., 2003, The First Two Decades of the Pu'u 'O'o-Kupaianaha Eruption: Chronology and Selected Bibliography: U.S. Geological Survey Professional Paper 1676, p. 1–27.

Ingersoll, R.V., 1979, Evolution of the Late Cretaceous forearc basin, northern and central California: Geological Society of America Bulletin, v. 90, Part I, p. 813–826, doi: 10.1130/0016-7606(1979)90<813:EOTLCF>2.0.CO;2.

Ingersoll, R.V., 1982, Initiation and evolution of the Great Valley forearc basin of northern and central California, USA, *in* Leggett, J.K., ed., Trench-Forearc Geology: Sedimentation and Tectonics on Modern and Ancient Active Plate Margins: Geological Society of London Special Publication 10, p. 459–467.

Jacobson, C.E., Grove, M., Barth, A.P., Pedrick, J.N., and Nourse, J.A., 2004, Detrital zircon geochronology indicates that Upper Cretaceous to Eocene sedimentary and metasedimentary rocks of Southern California, Salinia, and the Sur-Obispo terrane are not far traveled: Geological Society of America Abstracts with Programs, v. 36, no. 5, p. 511.

Jarrard, R.D., 1986, Terrane motion by strike-slip faulting of forearc slivers: Geology, v. 14, p. 780–783, doi: 10.1130/0091-7613(1986)14<780:TMBSFO>2.0.CO;2.

Kay, R.W., and Kay, S.M., 1991, Creation and destruction of the lower continental crust: Geologische Rundschau, v. 80, p. 259–270, doi: 10.1007/BF01829365.

Kidder, S., Ducea, M., Gehrels, G., Patchett, J., and Vervoort, J., 2003, Tectonic and magmatic development of the Salinian Coast Ridge belt, California: Tectonics, v. 22, no. 5, p. 1058, doi: 10.1029/2002TC001409.

Kistler, R.W., 1990, Two different types of lithosphere in the Sierra Nevada, California, *in* Anderson, J.L., ed., The Nature and Origin of Cordilleran Magmatism: Geological Society of America Memoir 174, p. 271–282.

Kistler, R.W., and Peterman, Z., 1973, Variations in Sr, Rb, K, Na, and initial $^{87}Sr/^{86}Sr$ in Mesozoic granitic rocks and intruded wallrocks in central California: Geological Society of America Bulletin, v. 84, p. 3489–3512, doi: 10.1130/0016-7606(1973)84<3489:VISRKN>2.0.CO;2.

Kistler, R.W., and Ross, D.C., 1990, A Strontium Isotopic Study of Plutons and Associated Rocks of the Southern Sierra Nevada and Vicinity, California: U.S. Geological Survey Bulletin 1920, 20 p.

Kistler, R.W., Chappell, B.W., Peck, D.L., and Bateman, P.C., 1986, Isotopic variation in the Tuolumne intrusive suite, central Sierra Nevada, California: Contributions to Mineralogy and Petrology, v. 94, p. 205–220, doi: 10.1007/BF00592937.

Klepeis, K.A., Clarke, G.L., and Rushmer, T., 2003, Magma transport and coupling between deformation and magmatism in the continental lithosphere: GSA Today, v. 13, p. 4–11, doi: 10.1130/1052-5173(2003)013<0004:MTACBD>2.0.CO;2.

Kokelaar, B.P., 1982, Fluidization of wet sediments during the emplacement and cooling of various igneous bodies: Journal of the Geological Society of London, v. 139, p. 21–33.

Krogh, T.E., 1982, Improved accuracy of U-Pb zircon ages by the creation of more concordant systems by an air abrasion technique: Geochimica et Cosmochimica Acta, v. 46, p. 637–649, doi: 10.1016/0016-7037(82)90165-X.

Lackey, J.S., Valley, J.W., and Saleeby, J.B., 2005, Supracrustal input to magmas in the deep crust of the Sierra Nevada batholith: Evidence from high-$\delta^{18}O$ zircon: Earth and Planetary Science Letters, v. 235, p. 315–330, doi: 10.1016/j.epsl.2005.04.003.

Lahren, M.M., and Schweickert, R.A., 1989, Proterozoic and Lower Cambrian miogeoclinal rocks of Snow Lake pendant, Yosemite-Emigrant Wilderness, Sierra Nevada, California: Evidence for major Early Cretaceous dextral translation: Geology, v. 17, p. 156–160, doi: 10.1130/0091-7613(1989)017<0156:PALCMR>2.3.CO;2.

Lee, C.-T., Yin, Q., Rudnick, R.L., Chesley, J.T., and Jacobsen, S.B., 2000, Re-Os isotopic evidence for pre-Miocene delamination of lithospheric mantle beneath the Sierra Nevada, California: Science, v. 289, p. 1912–1916, doi: 10.1126/science.289.5486.1912.

Ludwig, K.R., 2001, Users Manual for Isoplot/Ex (rev. 2.49): A Geological Toolkit for Microsoft Excel: Berkeley Geochronology Center Special Publication 1a, 56 p.

Mack, S., Saleeby, J.B., and Farrell, J.E., 1979, Origin and emplacement of the Academy pluton, Fresno County, California: Geological Society of America Bulletin, Part I, v. 90, p. 321–323; Part II, v. 90, p. 633–694.

Malin, P.E., Goodman, E.D., Henyey, T.L., Li, Y.-G., Okaya, D.A., and Saleeby, J.B., 1995, Significance of seismic reflections beneath a tilted exposure of deep continental crust, Tehachapi Mountains, California: Journal of Geophysical Research, v. 100, p. 2069–2087, doi: 10.1029/94JB02127.

Mansfield, C.F., 1979, Upper Mesozoic subsea fan deposits in the southern Diablo Range, California: Record of the Sierra Nevada magmatic arc: Geological Society of America Bulletin, v. 90, p. 1025–1046, doi: 10.1130/0016-7606(1979)90<1025:UMSFDI>2.0.CO;2.

Miller, W.J., and Webb, R.W., 1940, Descriptive geology of the Kernville Quadrangle, California: California Journal of Mines and Geology, v. 36, p. 343–378.

Nadin, E.S., 2007, Structure and history of the Kern Canyon fault system, southern Sierra Nevada, California [Ph.D dissertation]: Pasadena, California, California Institute of Technology, 288 p., 1 plate.

Nadin, E.S., and Saleeby, J.B., 2008, this volume, Disruption of regional primary structure of the Sierra Nevada batholith by the Kern Canyon fault system, California, *in* Wright, J.E., and Shervais, J.W., eds., Ophiolites, Arcs, and Batholiths: A Tribute to Cliff Hopson: Geological Society of America Special Paper 438, doi: 10.1130/2008.2438(15).

Paterson, S.R., Miller, R.B., Alsleben, H., Whitney, D.L., Valley, P.M., and Hurlow, H., 2008, 40–60 km of exhumation during Late Cretaceous contraction and Paleogene arc-oblique extension, Cascades core, Washington: Journal of Structural Geology (in press).

Pickett, D.A., and Saleeby, J.B., 1993, Thermobarometric constraints on the depth of the exposure and conditions of plutonism and metamorphism at deep levels of the Sierra Nevada batholith, Tehachapi Mountains, California: Journal of Geophysical Research, v. 98, p. 609–629.

Pickett, D.A., and Saleeby, J.B., 1994, Nd, Sr, and Pb isotopic characteristics of Cretaceous intrusive rocks from deep levels of the Sierra Nevada batholith, Tehachapi Mountains, California: Contributions to Mineralogy and Petrology, v. 118, p. 198–205, doi: 10.1007/BF01052869.

Pitcher, W.S., and Berger, A.R., 1972, The Geology of Donegal: A Study of Granite Emplacement and Unroofing: Regional Geology Series: New York, Wiley Interscience, 435 p.

Reid, S.A., and Cox, B.F., 1989, Early Eocene uplift of the southernmost San Joaquin basin, California: American Association of Petroleum Geology Bulletin, v. 73, p. 549.

Ross, D.C., 1989, The Metamorphic and Plutonic Rocks of the Southernmost Sierra Nevada, California and Their Tectonic Framework: U.S. Geological Survey Professional Paper 1381, 159 p., 2 plates.

Ross, D.C., 1995, Reconnaissance Geologic Map of the Southern Sierra Nevada, Kern, Tulare, and Inyo Counties, California: U.S. Geological Survey Miscellaneous Investigations Series Map I-2295, scale 1:125,000.

Ruppert, S., Fliedner, M.M., and Zandt, G., 1998, Thin crust and active upper mantle beneath the southern Sierra Nevada in the western United States: Tectonophysics, v. 286, p. 237–252.

Saleeby, J.B., 1981, Ocean floor accretion and volcanoplutonic arc evolution of the Mesozoic Sierra Nevada, California, *in* Ernst, W.G., ed., Rubey Volume on the Geotectonic Development of California: Englewood Cliffs, New Jersey, Prentice-Hall, p. 132–181.

Saleeby, J.B., 1990, Progress in tectonic and petrogenetic studies in an exposed cross-section of young (~100 Ma) continental crust, southern Sierra Nevada, California, *in* Salisbury, M.H., ed., Exposed Cross Sections of the Continental Crust: Dordrecht, Netherlands, D. Reidel Publishing, p. 137–158.

Saleeby, J.B., 2003, Segmentation of the Laramide slab-evidence from the southern Sierra Nevada region: Geological Society of America Bulletin, v. 115, p. 655–668, doi: 10.1130/0016-7606(2003)115<0655:SOTLSF>2.0.CO;2.

Saleeby, J.B., and Busby-Spera, C., 1986, Fieldtrip guide to the metamorphic framework rocks of the Lake Isabella area, southern Sierra Nevada, California, *in* Dunne, G.C., ed., Mesozoic and Cenozoic Structural Evolution of Selected Areas, East-Central California: Los Angeles, Geological Society of America, Cordilleran Section, Guidebook Volume, p. 81–94.

Saleeby, J.B., and Busby, C., 1993, Paleogeographic and tectonic setting of axial and western metamorphic framework rocks of the southern Sierra Nevada, California, *in* Dunne, G., and McDougall, K., eds., Mesozoic Paleogeography of the Western United States. Part II: Los Angeles, Pacific Section, Society of Economic Paleontologists and Mineralogists, Book 71, p. 197–226.

Saleeby, J.B., and Sharp, W.D., 1980, Chronology of the structural and petrologic development of the southwest Sierra Nevada Foothills, California: Geological Society of America Bulletin, Part I, v. 91, p. 317–320; Part II, v. 91, p. 1416–1535.

Saleeby, J.B., Busby, C., Goodin, W.D., and Sharp, W.D., 1978, Early Mesozoic paleotectonic-paleogeographic reconstruction of the southern Sierra Nevada region, California, *in* Howell, D., ed., Mesozoic Paleogeography of the Western United States: Los Angeles, Pacific Section, Society of Economic Paleontologists and Mineralogists, p. 311–336.

Saleeby, J.B., Sams, D.B., and Kistler, R.W., 1987, U/Pb zircon, strontium, and oxygen isotopic and geochronological study of the southernmost Sierra Nevada batholith, California: Journal of Geophysical Research, v. 92, p. 10,443–10,446.

Saleeby, J.B., Kistler, R.W., Longiaru, S., Moore, J.G., and Nokleberg, W.J., 1990, Middle Cretaceous silicic metavolcanic rocks in the Kings Canyon

area, central Sierra Nevada, California, *in* Anderson, J.L., ed., The Nature and Origin of Cordilleran Magmatism: Geological Society of America Memoir 174, p. 251–270.

Saleeby, J.B., Ducea, M., and Clemens-Knott, D., 2003, Production and loss of high-density batholithic root—Southern Sierra Nevada, California: Tectonics, v. 22, doi: 10.1029/2002TC001374.

Saleeby, J., Farley, K.A., Kistler, R.W., and Fleck, R., 2007, Thermal evolution and exhumation of deep-level batholithic exposures, southernmost Sierra Nevada, California, *in* Cloos, M., Carlson, W.D., Gilbert, M.C., Liou, J.G., and Sorensen, S.S., eds., Convergent Margin Terranes and Associated Regions: A Tribute to W.G. Ernst: Geological Society of America Special Paper 419, p. 39–66, doi: 10.1130/2007.2419(02)

Sisson, T.W., Grove, T.L., and Coleman, D.S., 1996, Hornblende gabbro sill complex at Onion Valley, California, and a mixing origin for the Sierra Nevada batholith: Contributions to Mineralogy and Petrology, v. 126, p. 81–108, doi: 10.1007/s004100050237.

Skilling, I.P., Busby, C.J., and Imai, T., 2004, Andesitic pepperite-bearing debris flows; physical volcanology and paleoenvironment of the Miocene Mehrten Formation, California: Geological Society of America Abstracts with Programs, v. 36, no. 4, p. 85.

Stern, T., Bateman, P.C., Morgan, B.A., Newell, M.F., and Peck, D.L., 1981, Isotopic U-Pb Ages of Zircon from the Granitoids of the Central Sierra Nevada, California: U.S. Geological Survey Professional Paper 1185, 17 p.

Tera, F., and Wasserburg, J.G., 1972, U/Pb systematics in lunar basalts: Earth and Planetary Science Letters, v. 17, p. 65–78, doi: 10.1016/0012-821X(72)90259-2.

Tikoff, B., and St. Blanquat, M., 1997, Transpressional shear and strike-slip partitioning in the Late Cretaceous Sierra Nevada magmatic arc, California: Tectonics, v. 16, p. 442–459, doi: 10.1029/97TC00720.

Tikoff, B., and Teyssier, C., 1992, Crustal-scale, en echelon P-shear tensional bridges—A possible solution to the batholithic room problem: Geology, v. 20, p. 927–930, doi: 10.1130/0091-7613(1992)020<0927:CSEEPS>2.3.CO;2.

Tobisch, O.T., Saleeby, J.B., and Fiske, R.S., 1986, Structural history of continental volcanic arc rocks along part of the eastern Sierra Nevada, California: A case for extensional tectonics: Tectonics, v. 5, p. 65–94.

Tobisch, O.T., Saleeby, J.B., Renne, P.R., McNulty, B., and Tong, W., 1995, Variations in deformation fields during development of a loarge volume magmatic arc, central Sierra Nevada, California: Geological Society of America Bulletin, v. 107, p. 148–166, doi: 10.1130/0016-7606(1995)107<0148:VIDFDD>2.3.CO;2.

Tobisch, O.T., Fiske, R.S., Saleeby, J.B., Holt, E., and Sorensen, S.S., 2000, Steep tilting of metavolcanic rocks by multiple mechanisms, central Sierra Nevada, California: Geological Society of America Bulletin, v. 112, no. 7, p. 1043–1058, doi: 10.1130/0016-7606(2000)112<1043:STOMRB>2.3.CO;2.

Wong, S.W., 2005, Structural Evolution of Mid-Crustal Shear Zones: Integrated Field and Thermochronologic Studies of the Sierra Mazatan Metamorphic Core Complex, Sonora, Mexico, and the Proto–Kern Canyon Dextral Shear Zone, Southern Sierra Nevada, California: [Ph.D. thesis]: Santa Barbara, University of California, 160 p.

Wood, D.J., and Saleeby, J.B., 1998, Late Cretaceous–Paleocene extensional collapse and disaggregation of the southernmost Sierra Nevada batholith: International Geology Review, v. 39, p. 973–1009.

Wood, D.J., and Saleeby, J., 2008, Structure and geochronology of the eastern Tehachapi Range, southernmost Sierra Nevada batholith, California: Geological Society of America Bulletin (in press).

Zeng, L., 2003, Non-modal partial melting of metasedimentary pendants in the southern Sierra Nevada and implications for the deep origin of within-pluton isotopic heterogeneity [Ph.D dissertation]: Pasadena, California, California Institute of Technology, 219 p., 1 plate.

Zeng, L., Saleeby, J., and Ducea, M., 2005, Geochemical characteristics of crustal anatexis during the formation of migmatite at the southern Sierra Nevada, California: Contributions to Mineralogy and Petrology, v. 150, p. 386–402, doi: 10.1007/s00410-005-0010-2.

Manuscript Accepted by the Society 16 July 2007